

Evaluation of a Direct Time Integration Scheme for Dynamic Analysis

by

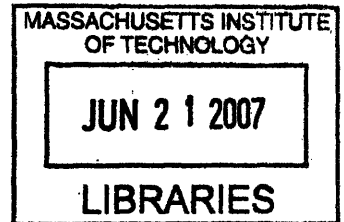
Jennifer D. Sanchez

SUBMITTED TO THE DEPARTMENT OF MECHANICAL ENGINEERING IN  
PARTIAL FULFILLMENT OF THE REQUIREMENTS FOR THE DEGREE OF

BACHELOR OF SCIENCE  
AT THE  
MASSACHUSETTS INSTITUTE OF TECHNOLOGY

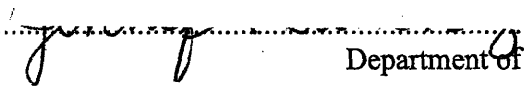
JUNE 2007

©2007 Jennifer D. Sanchez. All rights reserved.

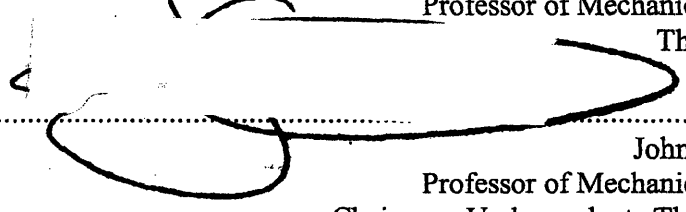


The author hereby grants to MIT permission to reproduce  
and to distribute publicly paper and electronic copies of this  
thesis document in whole or in part in any medium now  
known or hereafter created.

**ARCHIVES**

Signature of Author:  .....  
Department of Mechanical Engineering  
May 11, 2007

Certified by: .....  
Klaus-Jürgen Bathe  
Professor of Mechanical Engineering  
Thesis Supervisor

Accepted by:  .....  
John H. Lienhard V  
Professor of Mechanical Engineering  
Chairman, Undergraduate Thesis Committee

# Evaluation of a Direct Time Integration Scheme for Dynamic Analysis

by

Jennifer D. Sanchez

Submitted to the Department of Mechanical Engineering  
on May 11, 2007 in partial fulfillment of the  
requirements for the Degree of Bachelor of Science in  
Mechanical Engineering

## ABSTRACT

Direct integration schemes are important tools used in the dynamic analysis of many structures. It is critical that the solutions obtained from these schemes produce accurate results. Currently, one of the most widely used direct integration schemes is the trapezoidal rule. It is favored because it is a method that requires single steps and its results are second-order accurate. However, in cases where there are large deformations and longer integration times, the trapezoidal rule fails. A new composite method scheme shows promise in maintaining stability where the trapezoidal rule fails. It is a two step method that makes use of the trapezoidal rule and the three-point Euler backward method. The purpose of this study is to compare the trapezoidal rule and the new composite method using two nonlinear problems in order to determine if the composite method generates more accurate results than the trapezoidal rule.

Thesis Supervisor: Klaus-Jürgen Bathe  
Title: Professor of Mechanical Engineering

## **Acknowledgements**

I would like to acknowledge a few people who have contributed to the completion of this thesis. This has been a very challenging process and I have learned a great deal, not only in relation to direct time integration schemes but also organizational skills and independent study skills.

I would firstly like to acknowledge my thesis advisor, Professor Klaus-Jürgen Bathe, who guided me throughout this process. I greatly appreciated his encouragement and availability especially when considering his hectic schedule this semester.

I would also like to acknowledge each member of the Finite Element Research Group, especially Samar Malek. Thank you to all for offering a great environment to work in and always taking an interest and being helpful.

I would lastly like to thank MIT. I have learned and grown tremendously over these past four years and I feel like I am prepared for anything that I will encounter in my career. I will always look back fondly on the time that I have spent here and I consider myself blessed to have attended the best Institution in the world.

# Table of Contents

## **Chapter One          Introduction**

- 1.1 The need for dynamic analysis..... pg 8
- 1.2 Failures in a current analysis method and a proposed solution..... pg 8

## **Chapter Two          Dynamic equilibrium equations**

- 2.1 Equilibrium equations in linear analysis..... pg 9
- 2.2 Equilibrium equations in nonlinear analysis..... pg 9

## **Chapter Three        Time integration schemes and error evaluation**

- 3.1 Trapezoidal rule..... pg 11
- 3.2 Composite method..... pg 12
- 3.3 Error evaluation..... pg 13

## **Chapter Four        Numerical studies**

- 4.1 Large displacement analysis of a beam ..... pg 14
  - 4.1.1 Single pulse load function ..... pg 16
  - 4.1.2 Double pulse load function..... pg 25
  - 4.1.3 Triple pulse load function..... pg 30
- 4.2 Beam whip analysis ..... pg 35
  - 4.2.1 Obtaining an “exact” reference solution..... pg 36
  - 4.2.2 Single pulse load function ..... pg 38

## **Chapter Five        Conclusions ..... pg 41**

## Table of Figures and Tables

Figure 1: Problem1-Cantilevered Beam: This figure shows the geometrical set up of the first problem. The Young's Modulus $E = 2 \times 10^{11}$ Pa. The Poisson's ratio $\nu = 0.3$ . The thickness of the cantilever is 0.2m. The load $p$ is a time dependant pressure applied to the beam. Three different load functions were used in this analysis. They can be seen in Figures 2, 16, and 23.....	15
Figure 2: Load Function 1: This figure shows the first of three load functions $p$ used in this study. This load function was used in both problem.1 and problem 2. ....	16
Figure 3: Fourier Analysis of Acceleration-Composite Method-Load Function 1- 0.11s: This figure shows the results of the Fourier analysis run on problem 1 at time equal to 599.94 seconds using load function 1 and a time step of 0.11 seconds. The smallest mode frequency, 0.22 cycles/second, is the only frequency excited. ....	17
Figure 4: Fourier Analysis of Acceleration-Trapezoidal Rule-Load Function 1- 0.11s: This figure shows the results of the Fourier analysis run on problem 1 at a time equal to 536.8 seconds using load function 1 and a time step of 0.11 seconds. The smallest mode frequency, 0.22 cycles/seconds, is excited along with other frequencies. ....	17
Figure 5: Fourier Analysis of Acceleration-Composite Method-Load Function 1-0.22s: This figure shows the results of the Fourier analysis run on problem 1 at a time equal to 499.84 seconds using load function 1 and a time step of 0.22 seconds. The smallest mode frequency, 0.22 cycles/second, is the only frequency excited. ....	18
Figure 6: Fourier Analysis of Acceleration-Trapezoidal Rule-Load Function 1-0.22s: This figure shows the results of the Fourier analysis run on problem 1 at a time equal to 440.22 seconds using load function 1 and a time step of 0.22 seconds. The smallest mode frequency, 0.22 cycles/seconds, is excited along with other frequencies. ....	18
Figure 7: Load Function 1 Displacement: This figure shows that the tip of the cantilevered beam displaces about 2.5m. The displacements the beam experiences are 2.5 times its height. In addition, the trapezoidal rule and the composite method agree well with the reference data. ....	19
Figure 8: Load Function 1-Time Step 0.11s-Acceleration vs Time Plot: This figure shows that for a time step equal to 0.11s, the trapezoidal rule fails; whereas the composite method remains stable. ....	21
Figure 9: Load Function 1-Time Step 0.11s -Close Up: This figure shows the Acceleration vs Time plot seen in Figure 8 from 0 to 50 seconds. It shows that both the composite method and the trapezoidal rule obtain solutions similar to the exact solution. ....	21
Figure 10: Load Function 1-Time Step0.11s -Composite Method Percentage Total Error: This figure shows the percentage total error of the composite method as a function of time for a time step equal to 0.11s. ....	22
Figure 11: Load Function 1-Time Step 0.11s - Trapezoidal Rule Percentage Total Error: This figure shows the percentage total error of the trapezoidal rule as a function of time for a time step equal to 0.11s. The trapezoidal rule fails at time equal to 536.8s. ....	22

Figure 12: Load Function 1-Time Step 0.22s - Acceleration vs Time Plot: This figure shows that for a time step equal to 0.22s, the trapezoidal rule fails; whereas the composite method remains stable. ....	23
Figure 13: Load Function 1-Time Step 0.22s-Close Up: This figure shows the Acceleration vs Time plot seen in Figure 12 from 0 to 50 seconds. It shows that both the composite method and the trapezoidal rule obtain solutions similar to the exact solution. ....	23
Figure 14: Load Function 1-Time Step 0.22s -Composite Method Percentage Total Error: This figure shows the percentage total error of the composite method as a function of time for a time step equal to 0.22s. ....	24
Figure 15: Load Function 1-Time Step 0.22s-Trapezoidal Rule Percentage Total Error: This figure shows the percentage total error of the trapezoidal rule as a function of time for a time step equal to 0.22s. The trapezoidal rule fails at time equal to 440.2s. ....	24
Figure 16: Load Function 2: This figure shows the second load function $p$ applied to the cantilever beam. ....	25
Figure 17: Load Function 2-Time Step 0.11s-Acceleration vs Time Plot: This figure shows that for a time step equal to 0.11s, the trapezoidal rule fails; whereas the composite method remains stable. ....	26
Figure 18: Load Function 2-Time Step 0.11s-Composite Method Percentage Total Error: This figure shows the percentage total error of the composite method as a function of time for a time step equal to 0.11s. ....	27
Figure 19: Load Function 2-Time Step 0.11s-Trapezoidal Rule Percentage Total Error: This figure shows the percentage total error of the trapezoidal rule as a function of time for a time step equal to 0.11s. The trapezoidal rule fails at time equal to 181.8s. ....	27
Figure 20: Load Function 2-Time Step 0.22s-Acceleration vs Time Plot: This figure shows that for a time step equal to 0.22s, the trapezoidal rule fails; whereas the composite method remains stable. ....	28
Figure 21: Load Function 2-Time Step 0.22s-Composite Method Percentage Total Error: This figure shows the percentage total error of the composite method as a function of time for a time step equal to 0.22s. ....	29
Figure 22: Load Function 2-Time Step 0.22s-Trapezoidal Rule Percentage Total Error: This figure shows the percentage total error of the trapezoidal rule as a function of time for a time step equal to 0.22s. The trapezoidal rule fails at time equal to 138.6s. ....	29
Figure 23: Load Function 3: This figure shows the third load function $p$ applied to the cantilever beam. ....	30
Figure 24: Load Function 3-Time Step 0.11s-Acceleration vs Time Plot: This figure shows that for a time step equal to 0.11s, the trapezoidal rule fails; whereas the composite method remains stable. ....	31
Figure 25: Load Function 3-Time Step 0.11s-Composite Method Percentage Total Error: This figure shows the percentage total error of the composite method as a function of time for a time step equal to 0.11s. ....	32
Figure 26: Load Function 3-Time Step 0.11s-Trapezoidal Rule Percentage Total Error: This figure shows the percentage total error of the trapezoidal rule as a function of	

time for a time step equal to 0.11s. The trapezoidal rule fails at time equal to 387.6s. .....	32
Figure 27: Load Function 3-Time Step 0.22s-Acceleration vs Time Plot: This figure shows that for a time step equal to 0.22s, the trapezoidal rule fails; whereas the composite method remains stable. ....	33
Figure 28: Load Function 3-Time Step 0.22s-Composite Method Percentage Total Error: This figure shows the percentage total error of the composite method as a function of time for a time step equal to 0.22s. ....	34
Figure 29: Load Function 3-Time Step 0.22s-Trapezoidal Rule Percentage Total Error: This figure shows the percentage total error of the trapezoidal rule as a function of time for a time step equal to 0.22s. The trapezoidal rule fails at time equal to 365s. .....	34
Figure 30: Problem 2-Cantilevered Pipe Whip: This figure shows the geometrical set up of the second problem. The Young's Modulus $E$ , Poisson's ratio $\nu$ , and thickness of the cantilever remain the same as in the first problem. In this problem, the cantilever contacts a restraint that is 0.5m from it. The restraint is modeled as a truss whose Young's Modulus $E=2.5 \times 10^{11}$ Pa and face area equals $0.16\text{m}^2$ . The single pressure pulse $p$ as used in this problem. It can be seen in Figure 2.....	35
Figure 31: Beam Whip "Reference" Displacement: This figure shows the "reference" solutions calculated using different time steps for the displacement of the tip of the beam in problem 2.....	36
Figure 32: Beam Whip "Reference" Velocity: This figure shows the "reference" solutions calculated using different time steps for the velocity of the tip of the beam in problem 2.....	37
Figure 33: Beam Whip "Reference" Acceleration: This figure shows the "reference" solutions calculated using different time steps for the acceleration of the tip of the beam in problem 2.....	37
Figure 34: Beam Whip-Time Step 0.11s-Displacement vs Time Plot: This figure shows the displacement solutions obtained for the tip of the beam by using a time step of 0.0044s for the "Reference" solution and 0.11s for the other schemes.....	39
Figure 35: Beam Whip-Time Step 0.11s-Velocity vs Time Plot: This figure shows the velocity solutions obtained for the tip of the beam by using a time step of 0.0044s for the "Reference" solution and 0.11s for the other schemes.....	39
Figure 36: Beam Whip-Time Step 0.11s-Acceleration vs Time Plot: This figure shows the acceleration solutions obtained for the tip of the beam by using a time step of 0.0044s for the "Reference" solution and 0.11s for the other schemes.....	40
 Table 1: Mode Frequencies and Periods: This table lists the first six mode frequencies and periods of the cantilevered beam at zero displacements shown in Figure 1. ....	15

# **Chapter One: Introduction**

## **1.1 The need for dynamic analysis**

Dynamic analysis is an important tool that helps engineers to design and develop structures that will be exposed to dynamic loads throughout their lifetime. Direct time integration schemes used in dynamic analysis help to identify critical loads, materials, and geometries that may lead to a failure in structures. The accuracy that the direct time integration schemes can produce is very important. Greater accuracy provides more opportunity for engineers to design structures to fit their requirements. This can help to reduce costs of structures, reduce time in building structures, and in the cases of bridges, tunnels, or buildings maintain the safety of the people using the structures.

## **1.2 Failures in a current analysis method and a proposed solution**

The trapezoidal rule, a special case of the Newmark method, is currently one of the most widely used implicit direct time integration schemes in structural vibration analysis. It is valuable because it is a method that requires single steps and its results are second-order accurate. However, for conditions where large deformations occur and long time integrals are required, the trapezoidal rule becomes unstable.

A new composite time integration method has been proposed that hopes to produce accurate results where the trapezoidal rule fails. It is a two step scheme that utilizes both the trapezoidal rule and the three-point Euler backward method.

The purpose of this study is to determine if the composite scheme is better than the trapezoidal rule when large deformations occur and long time integrals are required. This will be tested by comparing the amount of computational effort required and the accuracy of the acceleration solutions generated for each method. The methods will be compared by using two nonlinear problems, multiple load functions, and different integration steps.



## Chapter Two: Dynamic Equilibrium Equations

### 2.1 Equilibrium equations in linear analysis

In linear analysis, the boundary conditions for the structure remain constant throughout the analysis, the displacements are small, and the structure's materials are linearly elastic. The equilibrium equations for linear dynamic analysis are

$$\mathbf{M}\ddot{\mathbf{U}} + \mathbf{C}\dot{\mathbf{U}} + \mathbf{K}\mathbf{U} = \mathbf{R} \quad (1)$$

where  $\mathbf{M}$  is the mass matrix,  $\mathbf{C}$  is the damping matrix,  $\mathbf{K}$  is the stiffness matrix,  $\mathbf{R}$  is the vector of externally applied nodal point forces,  $\ddot{\mathbf{U}}$  is the vector of nodal accelerations,  $\dot{\mathbf{U}}$  is the vector of nodal velocities, and  $\mathbf{U}$  is the vector of nodal displacements.

### 2.2 Equilibrium equations in nonlinear analysis

In nonlinear analysis, the boundary conditions of the structure may change over time, the displacements may be large, and the materials may not be linearly elastic. The equilibrium equations for a nonlinear implicit time integration dynamic analysis are found by examining the conditions that must hold throughout the nonlinear analysis. This condition is [1]

$$\mathbf{R} - \mathbf{F} = \mathbf{M}\ddot{\mathbf{U}} \quad (2)$$

where  $\mathbf{M}$ ,  $\ddot{\mathbf{U}}$ , and  $\mathbf{R}$  have been previously defined,  $\mathbf{F}$  is the vector of nodal point forces due to stresses in individual elements of the structure, and any damping given by  $\mathbf{C}\dot{\mathbf{U}}$  is neglected. The equilibrium equations must be solved over the complete range of time in the analysis. The solution to the equilibrium at time step  $t$  is considered to be known. These solutions are used to evaluate the equilibrium at the time step  $t + \Delta t$ . The solution at this time step is used to find the solution at the following time step and so on. The equilibrium equations are

$${}^{t+\Delta t}\mathbf{R} - {}^{t+\Delta t}\mathbf{F} = \mathbf{M}{}^{t+\Delta t}\ddot{\mathbf{U}} \quad (3)$$

The equations for nodal point forces at time  $t + \Delta t$  are

$${}^{t+\Delta t}\mathbf{F} = {}^t\mathbf{F} + \mathbf{F} \quad (4)$$

where  $\mathbf{F}$  is the vector of nodal point forces that are achieved over the time period  $\Delta t$  due to stresses in individual elements. This change in nodal point forces can be determined using the equation

$$\mathbf{F} = {}^t\mathbf{K}\mathbf{U} \quad (5)$$

where  ${}^t\mathbf{K}$  is the stiffness matrix at time  $t$  and  $\mathbf{U}$  is the vector of incremental nodal displacements. Combining equations (3), (4), and (5) produces

$$\mathbf{M}{}^{t+\Delta t}\ddot{\mathbf{U}} + {}^t\mathbf{K}\mathbf{U} = {}^{t+\Delta t}\mathbf{R} - {}^t\mathbf{F} \quad (6)$$

where  $\mathbf{U}$  is the approximation of the change in the vector of nodal displacements over the time period  $\Delta t$ . Therefore, an approximation of  ${}^{t+\Delta t}\mathbf{U}$  can be determined using

$${}^{t+\Delta t}\mathbf{U} \doteq {}^t\mathbf{U} + \mathbf{U} \quad (7)$$

where  ${}^t\mathbf{U}$  is the known nodal displacement at time  $t$ . The iterative method known as the Newton-Raphson technique uses this approach repetitively at time  $t + \Delta t$  to converge upon the solution of the nodal displacements, velocities, and accelerations. The Newton-Raphson technique will be used when carrying out the trapezoidal rule and the new composite method scheme [1].

## Chapter Three: Time Integration Schemes and Error Evaluation

In direct time integration schemes, the equilibrium equations are evaluated at different time steps and all solutions prior to and including the time point  $t$  are considered to be known. These direct time integration schemes provide the solutions of nodal displacements, velocities, and accelerations at times  $\Delta t$  apart [1, 2].

### 3.1 Trapezoidal rule

The trapezoidal rule is a special case of the Newmark method. The Newmark method is a single step method that uses parameters  $\alpha$  and  $\delta$  in its equations to gain the best stability and accuracy in its solutions. Its equations for nodal displacements and velocities at time  $t + \Delta t$  are

$${}^{t+\Delta t}\mathbf{U} = {}^t\mathbf{U} + {}^t\dot{\mathbf{U}}\Delta t + \left[\left(\frac{1}{2} - \alpha\right)\ddot{\mathbf{U}} + \alpha {}^{t+\Delta t}\ddot{\mathbf{U}}\right]\Delta t^2 \quad (8)$$

$${}^{t+\Delta t}\dot{\mathbf{U}} = {}^t\dot{\mathbf{U}} + \left[(1 - \delta)\ddot{\mathbf{U}} + \delta {}^{t+\Delta t}\ddot{\mathbf{U}}\right]\Delta t \quad (9)$$

where  $\mathbf{U}$ ,  $\dot{\mathbf{U}}$ ,  $\ddot{\mathbf{U}}$ ,  $\alpha$ ,  $\delta$  have been previously defined. The superscripts preceding  $\mathbf{U}$ ,  $\dot{\mathbf{U}}$ , and  $\ddot{\mathbf{U}}$  refer to the time at which these displacements, velocities, and accelerations occur. The Newmark method becomes the trapezoidal rule when  $\alpha = \frac{1}{4}$  and  $\delta = \frac{1}{2}$ . Therefore, its equations for displacements and velocities at time  $t + \Delta t$  become

$${}^{t+\Delta t}\mathbf{U} = {}^t\mathbf{U} + \left[\frac{\Delta t}{2}\right]({}^t\dot{\mathbf{U}} + {}^{t+\Delta t}\dot{\mathbf{U}}) \quad (10)$$

$${}^{t+\Delta t}\dot{\mathbf{U}} = {}^t\dot{\mathbf{U}} + \left[\frac{\Delta t}{2}\right]({}^t\ddot{\mathbf{U}} + {}^{t+\Delta t}\ddot{\mathbf{U}}) \quad (11)$$

An iterative scheme must be used to evaluate the nodal displacements and velocities for equations (10) and (11). The Newton-Raphson iteration may be used. Its equations for  $i = 1, 2, 3, \dots$  are

$${}^{t+\Delta t}\mathbf{U}^{(i)} = {}^{t+\Delta t}\mathbf{U}^{(i-1)} + \Delta\mathbf{U}^{(i)} \quad (12)$$

$$\Delta \mathbf{U}^{(i)} = {}^{t+\Delta t} \mathbf{U}^{(i)} - {}^{t+\Delta t} \mathbf{U}^{(i-1)} \quad (13)$$

These equations used in conjunction with the equilibrium equations of the dynamic problem allow convergence upon the displacements, velocities, and accelerations at time  $t + \Delta t$  [1].

### 3.2 Composite method

The Composite method is a two step method that uses the trapezoidal rule for its first sub-step and the three-point Euler backward method for its second sub-step [3, 4]. It uses the trapezoidal rule to find the solutions for nodal displacements, velocities, and accelerations at time  $t + \gamma \Delta t$ . Then it uses the solutions from its first sub-step to find the solutions at time  $t + \Delta t$  using the three-point Euler backward method. The Euler backward method equations are

$${}^{t+\Delta t} \dot{\mathbf{U}} = \mathbf{c}_1 {}^t \mathbf{U} + \mathbf{c}_2 {}^{t+\gamma \Delta t} \mathbf{U} + \mathbf{c}_3 {}^{t+\Delta t} \mathbf{U} \quad (14)$$

$${}^{t+\Delta t} \ddot{\mathbf{U}} = \mathbf{c}_1 {}^t \dot{\mathbf{U}} + \mathbf{c}_2 {}^{t+\gamma \Delta t} \dot{\mathbf{U}} + \mathbf{c}_3 {}^{t+\Delta t} \dot{\mathbf{U}} \quad (15)$$

where

$$\mathbf{c}_1 = \frac{(1-\gamma)}{\gamma \Delta t} \quad (16)$$

$$\mathbf{c}_2 = \frac{-1}{(1-\gamma)\gamma \Delta t} \quad (17)$$

$$\mathbf{c}_3 = \frac{(2-\gamma)}{(1-\gamma)\Delta t} \quad (18)$$

In this analysis, the sub-steps will be of magnitude  $\frac{\Delta t}{2}$ . Therefore, the Euler backward method equations use  $\gamma = \frac{1}{2}$ . The Euler equations become

$${}^{t+\Delta t} \dot{\mathbf{U}} = \frac{1}{\Delta t} {}^t \mathbf{U} - \frac{4}{\Delta t} {}^{t+\Delta/2} \mathbf{U} + \frac{3}{\Delta t} {}^{t+\Delta t} \mathbf{U} \quad (19)$$

$${}^{t+\Delta t}\ddot{U} = \frac{1}{\Delta t} {}^t\dot{U} - \frac{4}{\Delta t} {}^{t+\Delta t/2}\dot{U} + \frac{3}{\Delta t} {}^{t+\Delta t}\dot{U} \quad (20)$$

Equations (19) and (20) are used along with the equilibrium equation and the results of using the trapezoidal rule in the first sub-step at time  $t + \frac{\Delta t}{2}$  to obtain the nodal displacements, velocities, and accelerations at time  $t + \Delta t$ .

### 3.3 Error evaluation

The error for each method was calculated by obtaining an “exact” reference solution of each problem and calculating the mean square error of each method as it compared to the reference solution. The equation to obtain the mean square error is

$$\text{MSE} = \frac{1}{n} \sum_{j=1}^n (\theta_j - \theta)^2 \quad (21)$$

where  $n$  is the number of steps,  $\theta$  is the reference solution, and  $\theta_j$  is a solution obtained from either the trapezoidal rule or the composite method. The **MSE** provides the mean square value of the error magnitude considering all time steps 1 to  $n$ . The root mean square error, **RMSE**, provides the magnitude of the error seen in the amplitude of the data. The **RMSE** of a data set can be obtained using the equation

$$\text{RMSE} = \sqrt{\text{MSE}} \quad (22)$$

The **RMSE** can be normalized by using the maximum magnitude of the reference solution to find the percentage error. This can be seen in the equation

$$\text{Error} = \frac{\text{RMSE}}{\text{Val}_{\max}} \times 100\% \quad (23)$$

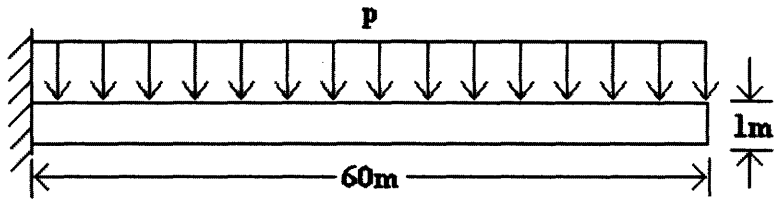
where  $\text{Val}_{\max}$  is the maximum magnitude seen in the reference solution.

## Chapter Four: Numerical Studies

Two nonlinear structural problems were selected to compare the trapezoidal rule and the new composite method. One problem focused on large displacements and the other focused on physical interaction with another object. The conditions in each of the problems were consistent with those that normally lead to a failure in the trapezoidal rule: large displacements and long time integrals. This was done with the intention of learning whether the composite rule is better than the trapezoidal rule under these conditions. In addition, three separate load functions and two different time steps were used in this study. The finite element analysis computer program ADINA was used to acquire solutions for nodal displacements, velocities, and accelerations in addition to running Fourier analysis for each method. The computer program MATLAB was used to calculate the percentage total error in the large displacements problem for all cases.

### 4.1 Large displacement analysis of a beam

The first problem evaluated was the cantilevered beam shown in Figure 1. The first six mode frequencies and periods for this beam may be seen in Table 1. This beam was subjected to the three different loading functions  $\mathbf{p}$  (a single pulse, a double pulse, and a triple pulse) shown in Figures 2, 16, and 23. The beam was divided into sixty nine-node plane stress elements. In addition, two different integration time steps were used: 0.11 seconds and 0.22 seconds. These time steps correspond to 1/40 and 1/20 of the smallest mode period (4.4 seconds) respectively calculated for the beam. A time step of 0.0044 seconds (1/1000 of the smallest mode period) was used to create an “exact” reference solution. In addition, the beam material was modeled as an elastic isotropic material whose Young’s Modulus  $\mathbf{E} = 2 \times 10^{11}$  Pa and Poisson’s ratio  $\nu = 0.3$ . The yield stress in this case was  $\sigma_y = 2 \times 10^8$  Pa and the effective stress was  $\sigma_e = 4.49 \times 10^7$  Pa. Additionally, the convergence tolerance criterion set in this analysis required that the energy for each iteration must have converged to within  $10^{-8}$  J of the original energy increment and the force for each iteration must have converged to within  $10^{-6}$  N of the original force increment.



**depth = 0.2m**                      **plane stress**  
**Poisson's Ratio  $\nu = 0.3$**                       **sixty 9-node elements**  
**Young's Modulus  $E = 2 \times 10^{11}$  Pa**

**Figure 1: Problem1-Cantilevered Beam:** This figure shows the geometrical set up of the first problem. The Young's Modulus  $E = 2 \times 10^{11}$  Pa. The Poisson's ratio  $\nu = 0.3$ . The thickness of the cantilever is 0.2m. The load  $p$  is a time dependant pressure applied to the beam. Three different load functions were used in this analysis. They can be seen in Figures 2, 16, and 23.

Mode	Frequency [Rad/s]	Frequency [Cycles/s]	Period [s]
1	0.1423E+01	0.2265E+00	0.4414E+01
2	0.8910E+01	0.1418E+01	0.7051E+00
3	0.2490E+02	0.3964E+01	0.2523E+00
4	0.4867E+02	0.7747E+01	0.1291E+00
5	0.8019E+02	0.1276E+02	0.7836E-01
6	0.1193E+03	0.1899E+02	0.5267E-01

**Table 1: Mode Frequencies and Periods:** This table lists the first six mode frequencies and periods of the cantilevered beam at zero displacements shown in Figure 1.

### 4.1.1 Single pulse load function

The first load function (load function 1) used in this study was a single pressure pulse that started at  $t = 0$  seconds, peaked at  $t = 2$  seconds, and ended at  $t = 4$  seconds. It can be seen in Figure 2. The peak pressure used was 18kPa. The pressure applied to the beam at any time  $t > 4$  seconds was zero. This load function 1 was used again in problem 2 (beam whip analysis).

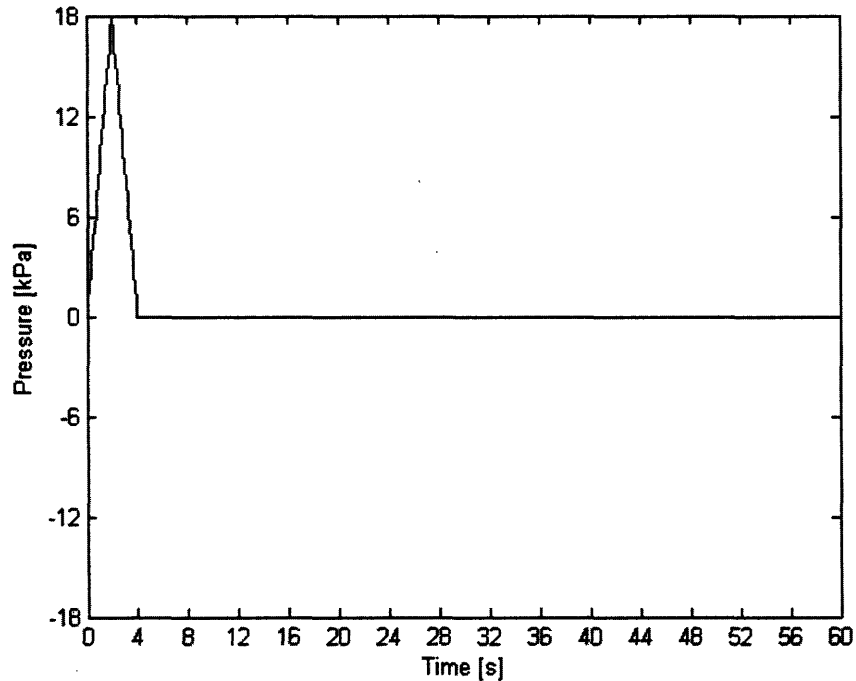


**Figure 2: Load Function 1:** This figure shows the first of three load functions  $p$  used in this study. This load function was used in both problem 1 and problem 2.

In order to determine if the time steps  $\Delta t$  (0.11 seconds and 0.22 seconds) used in this study were small enough to detect this load function, a Fourier analysis for acceleration was completed at the final time iteration of each method to determine if the smallest mode frequency (0.22 cycles/second) was excited. The results of this analysis for the composite method and the trapezoidal rule can be seen in Figures 3, 4, 5, and 6. These figures show that for the composite method, the smallest mode frequency is the only frequency that is excited for both time steps. The Fourier analysis shows the complete failure that the trapezoidal rule experiences with a drastic increase in the amplitude at a frequency other than the smallest mode frequency. In addition, the Fourier analysis



shows that the trapezoidal rule is also excited by the smallest mode frequency. However, this magnitude is much smaller than the other frequencies that appear to be excited as seen in Figure 6. When  $\Delta t = 0.11$  seconds, the difference in magnitudes is so great that the peak representing the smallest mode frequency is not visible (Figure 4).

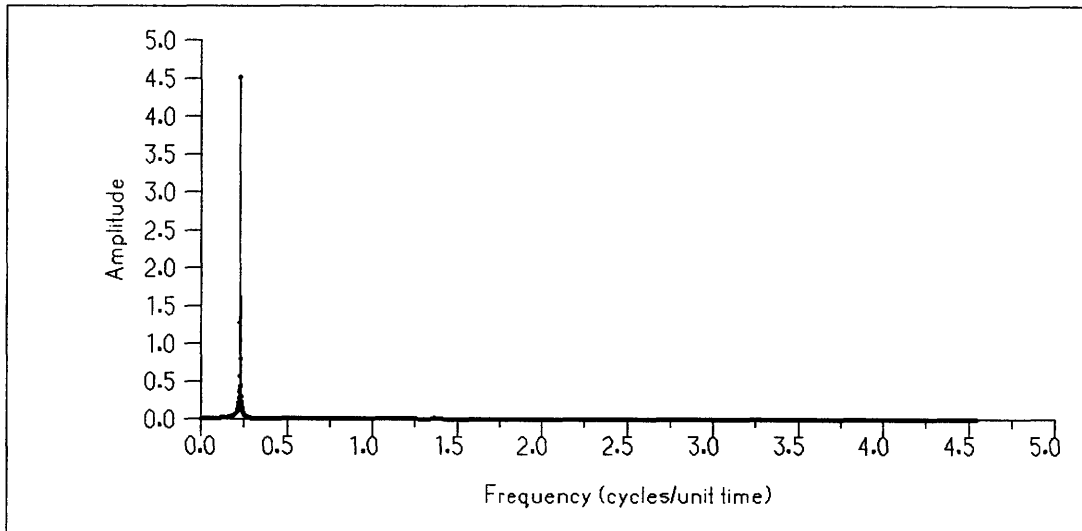


**Figure 3: Fourier Analysis of Acceleration-Composite Method-Load Function 1-0.11s:** This figure shows the results of the Fourier analysis run on problem 1 at time equal to 599.94 seconds using load function 1 and a time step of 0.11 seconds. The smallest mode frequency, 0.22 cycles/second, is the only frequency excited.

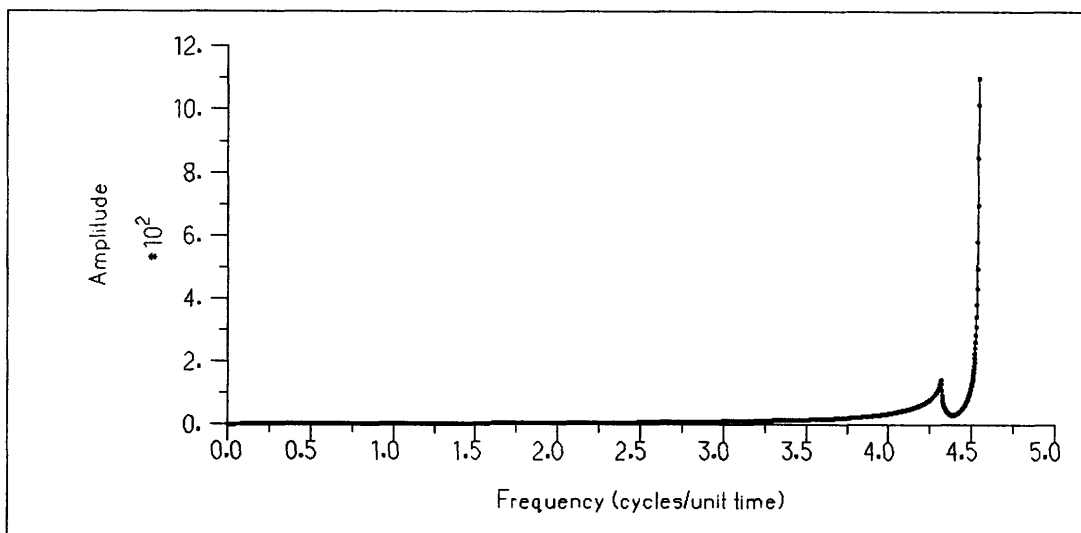


**Figure 4: Fourier Analysis of Acceleration-Trapezoidal Rule-Load Function 1-0.11s:** This figure shows the results of the Fourier analysis run on problem 1 at a time equal to 536.8 seconds using load function 1 and a time step of 0.11 seconds. The smallest mode frequency, 0.22 cycles/seconds, is excited along with other frequencies.

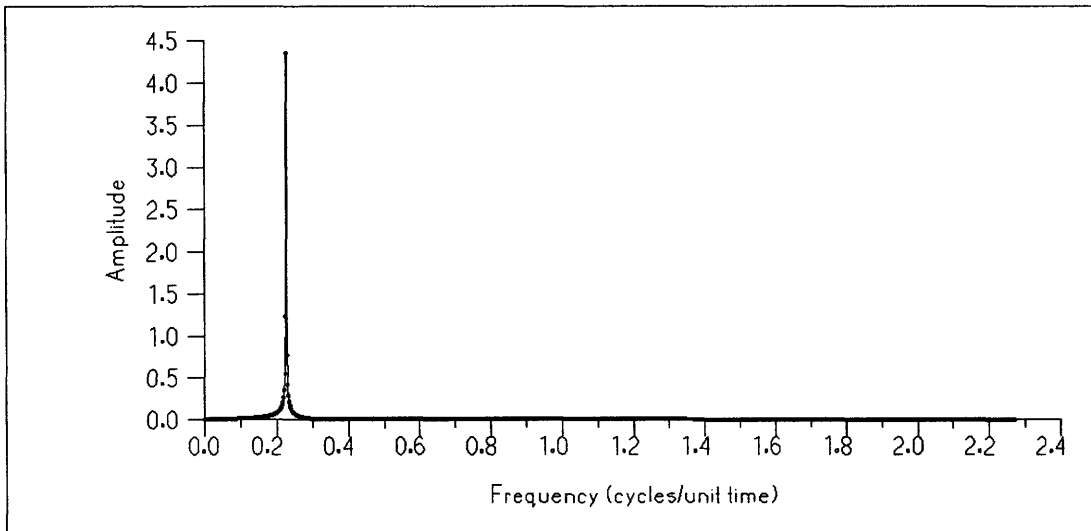


**Figure 5: Fourier Analysis of Acceleration-Composite Method-Load Function 1-0.22s:** This figure shows the results of the Fourier analysis run on problem 1 at a time equal to 499.84 seconds using load function 1 and a time step of 0.22 seconds. The smallest mode frequency, 0.22 cycles/second, is the only frequency excited.

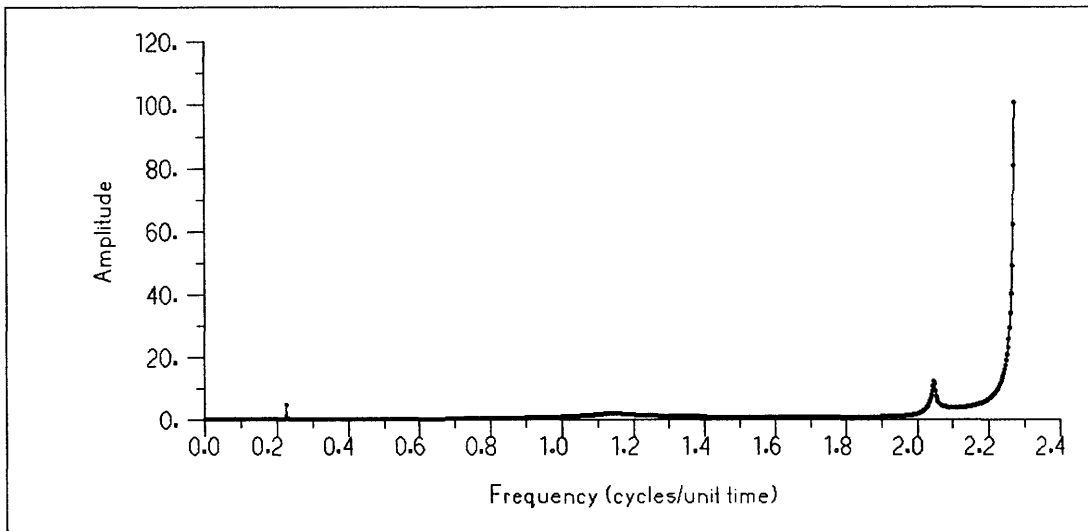


**Figure 6: Fourier Analysis of Acceleration-Trapezoidal Rule-Load Function 1-0.22s:** This figure shows the results of the Fourier analysis run on problem 1 at a time equal to 440.22 seconds using load function 1 and a time step of 0.22 seconds. The smallest mode frequency, 0.22 cycles/seconds, is excited along with other frequencies.

The trapezoidal rule and the composite method were each used to find the displacement of the tip of the beam as a function of time resulting from load function 1. The solutions were found using the time step 0.11 seconds. In addition, an “exact solution” for the displacement and the acceleration at the tip of the beam was obtained by using the composite method with a time step of 0.0044 seconds (1/1000 of the smallest mode period). The displacement solution found for each scheme and the reference solution can be seen in Figure 7. This figure displays the scale of the large displacements seen by the beam.

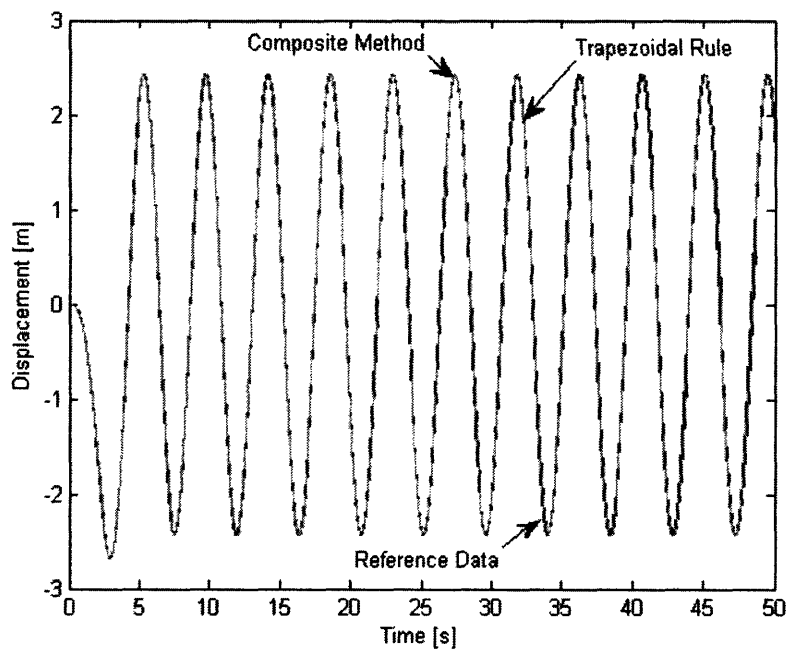


**Figure 7: Load Function 1 Displacement:** This figure shows that the tip of the cantilevered beam displaces about 2.5m. The displacements the beam experiences are 2.5 times its height. In addition, the trapezoidal rule and the composite method agree well with the reference data.

The acceleration solution for the tip of the beam in this case was found in the same way as the displacement solution. Another time step, 0.22 seconds, was used in addition to 0.11 seconds. The acceleration solution for the time step 0.11 seconds can be seen in Figure 8. In this case, the trapezoidal rule fails at time  $t = 536.8$  seconds and the composite method remains stable. The reference data cannot be seen due to the scale of

the trapezoidal rule's failure. The composite method's data line covers it up since they are of the same magnitude. The acceleration solution obtained with the trapezoidal rule is also of the same magnitude initially. This can be seen in Figure 9. However, neither method matches the reference data exactly. There is some error in both schemes. These errors were measured by calculating the root mean square error of the acceleration magnitudes found for each scheme and the reference data. The percentage total error was obtained by normalizing the error data by dividing through by the maximum acceleration magnitude found in the reference data. The percentage total error results for each scheme can be seen in Figures 10 and 11.

The error analysis shows that while the error in the composite method increases steadily over time, the error in the trapezoidal rule can quickly reach magnitudes that are greater than 16,000% of the maximum acceleration magnitude found in the exact solution before failing.

The analysis for problem 1 was completed a second time using a time step of 0.22 seconds. The acceleration solutions for each scheme in this case can be seen in Figure 12. The behavior observed using time step 1 can be seen in this case as well. The trapezoidal rule fails at time  $t = 440.2$  seconds while the composite method remains stable. The percentage total error for the composite method using a time step of 0.22 seconds is greater than the percentage total error found using a time step of 0.11 seconds because of the increase in the magnitude of the time step. Since the time step is larger, the acceleration solution is not as exact and the error increases. The trapezoidal rule fails at an earlier time in this case for the same reason.

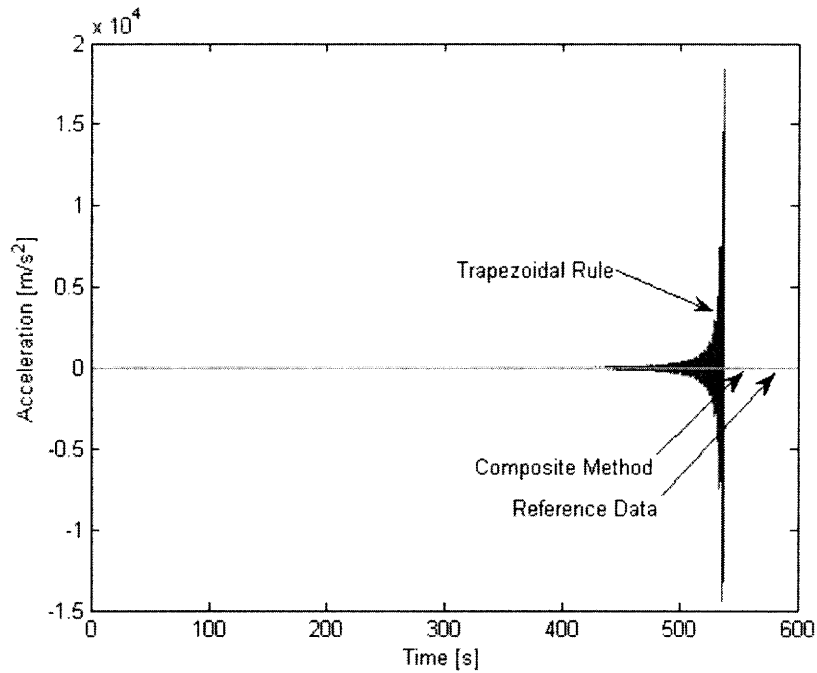


**Figure 8: Load Function 1-Time Step 0.11s-Acceleration vs Time Plot:** This figure shows that for a time step equal to 0.11s, the trapezoidal rule fails; whereas the composite method remains stable.

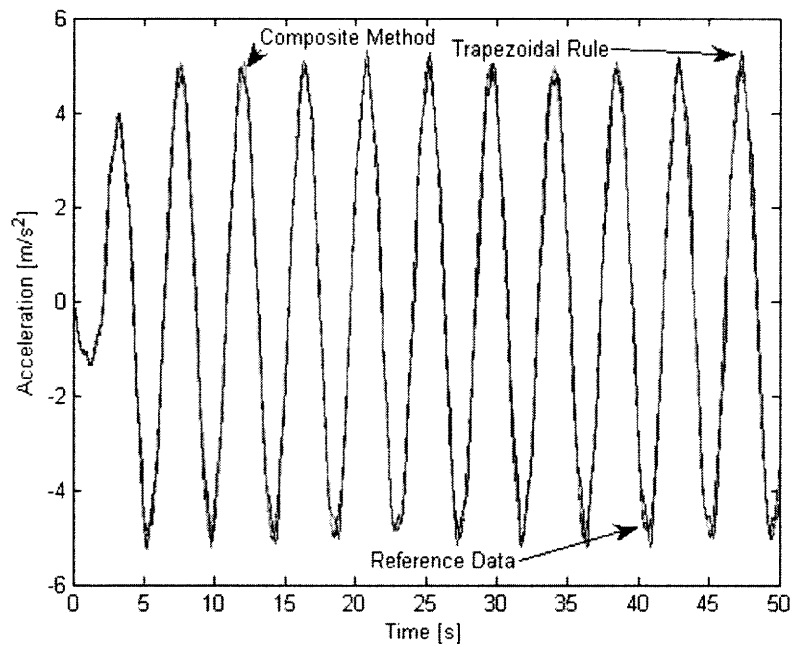


**Figure 9: Load Function 1-Time Step 0.11s -Close Up:** This figure shows the Acceleration vs Time plot seen in Figure 8 from 0 to 50 seconds. It shows that both the composite method and the trapezoidal rule obtain solutions similar to the exact solution.

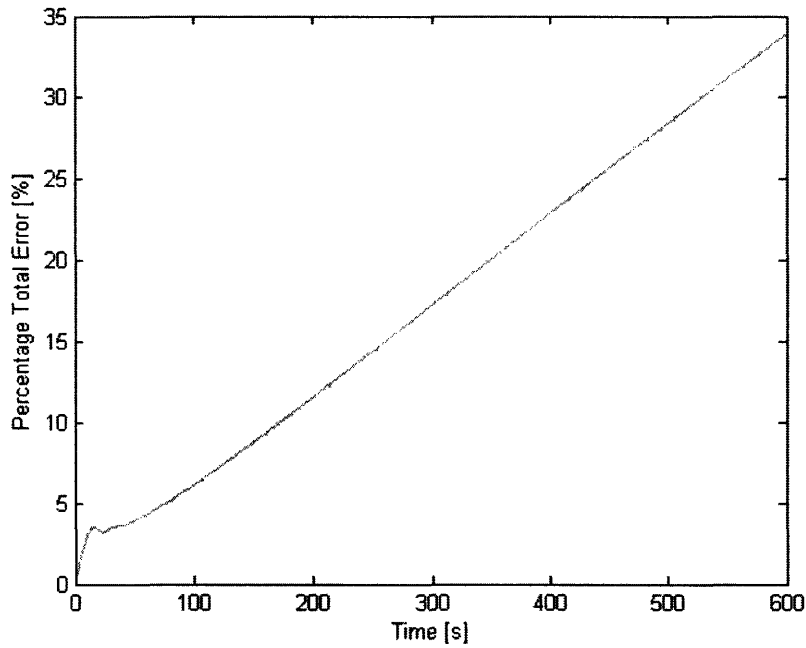


**Figure 10: Load Function 1-Time Step 0.11s -Composite Method Percentage Total Error:** This figure shows the percentage total error of the composite method as a function of time for a time step equal to 0.11s.

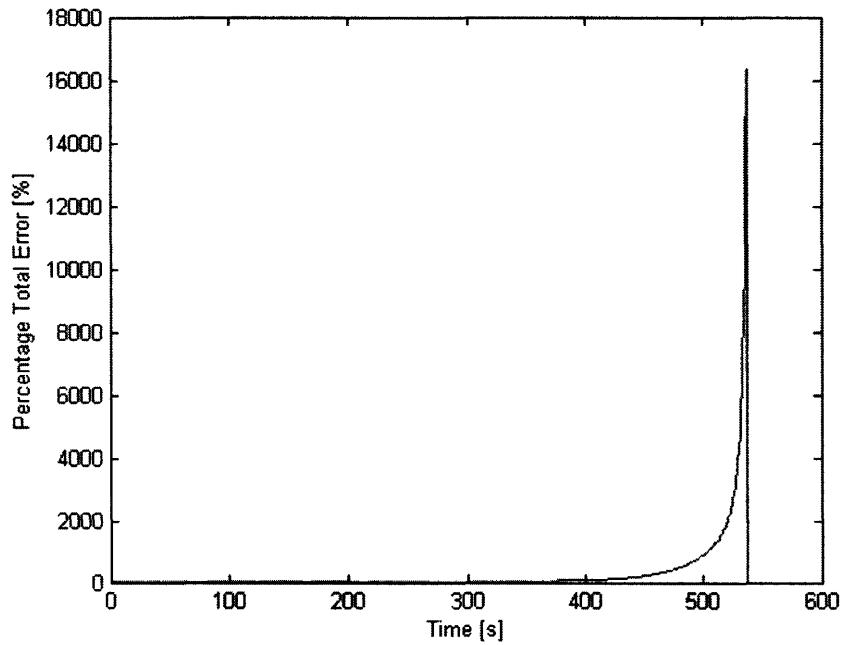


**Figure 11: Load Function 1-Time Step 0.11s - Trapezoidal Rule Percentage Total Error:** This figure shows the percentage total error of the trapezoidal rule as a function of time for a time step equal to 0.11s. The trapezoidal rule fails at time equal to 536.8s.

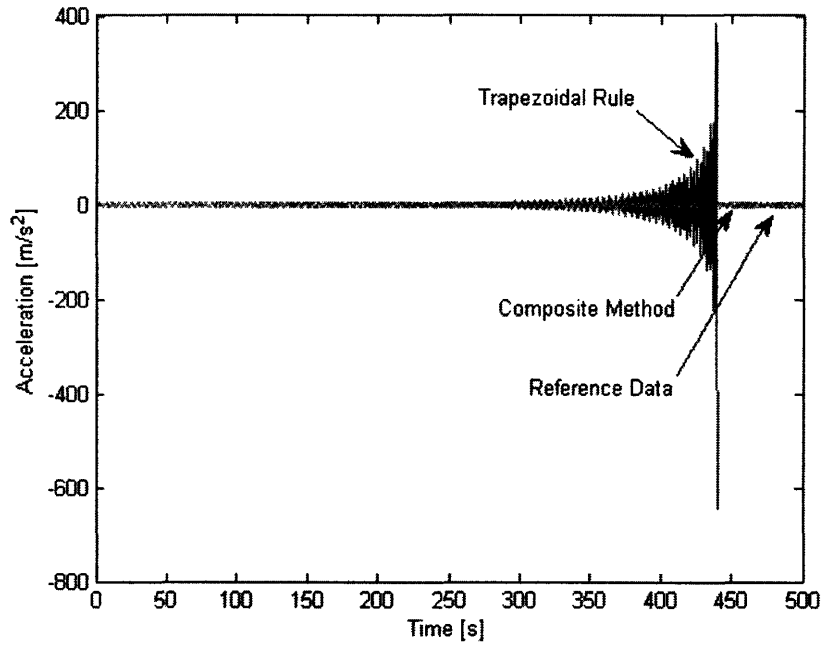


**Figure 12: Load Function 1-Time Step 0.22s - Acceleration vs Time Plot:** This figure shows that for a time step equal to 0.22s, the trapezoidal rule fails; whereas the composite method remains stable.

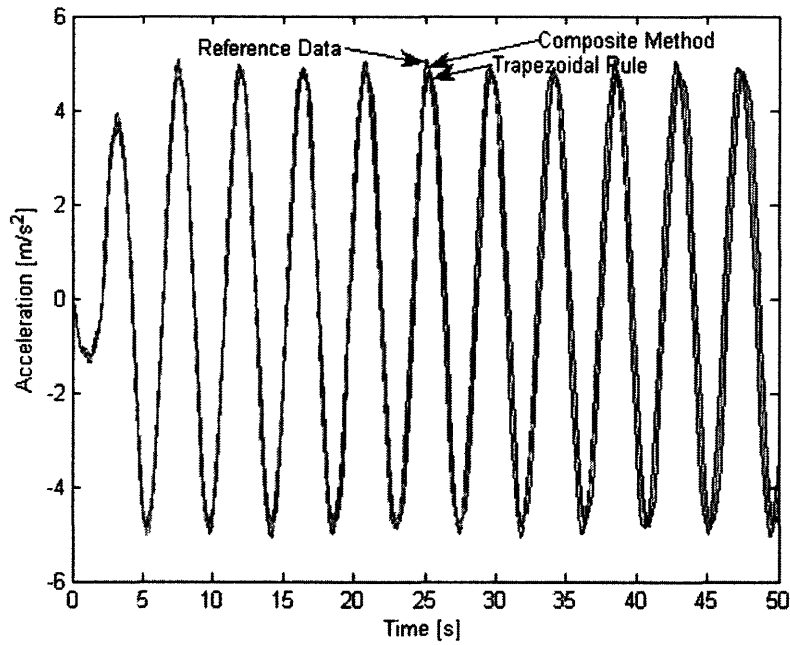


**Figure 13: Load Function 1-Time Step 0.22s-Close Up:** This figure shows the Acceleration vs Time plot seen in Figure 12 from 0 to 50 seconds. It shows that both the composite method and the trapezoidal rule obtain solutions similar to the exact solution.

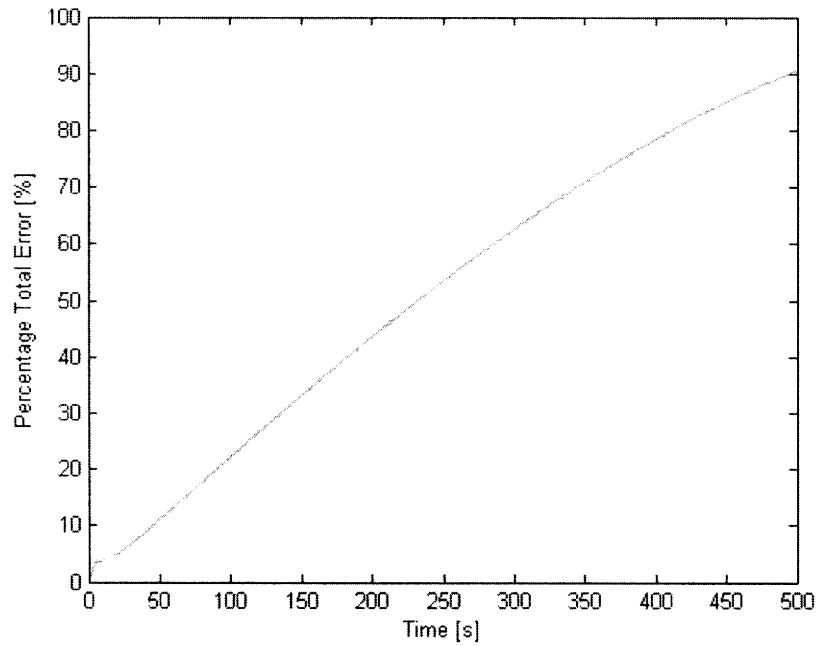


**Figure 14: Load Function 1-Time Step 0.22s -Composite Method Percentage Total Error:** This figure shows the percentage total error of the composite method as a function of time for a time step equal to 0.22s.

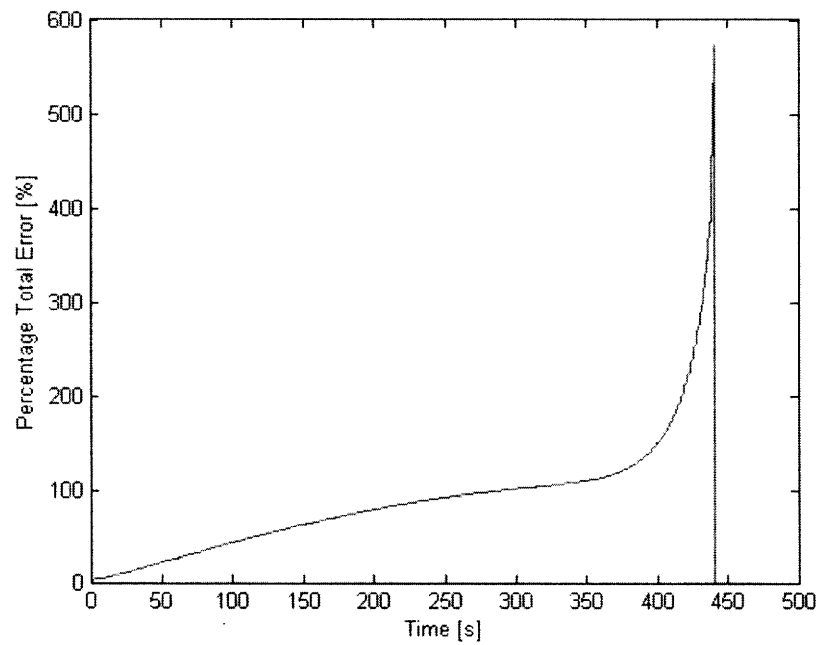


**Figure 15: Load Function 1-Time Step 0.22s-Trapezoidal Rule Percentage Total Error:** This figure shows the percentage total error of the trapezoidal rule as a function of time for a time step equal to 0.22s. The trapezoidal rule fails at time equal to 440.2s.



#### 4.1.2 Double pulse load function

The second load function (load function 2) used in this study was a double pressure pulse whose peaks were separated by 18 seconds. The first pressure pulse was identical to the one seen in load function 1. The second pressure pulse started at  $t = 18$  seconds, peaked at  $t = 20$  seconds, and ended at  $t = 22$  seconds. Load function 2 can be seen in Figure 16. The peak pressure in each pulse was 18kPa. The pressure applied to the beam at any time  $t > 22$  seconds was zero.

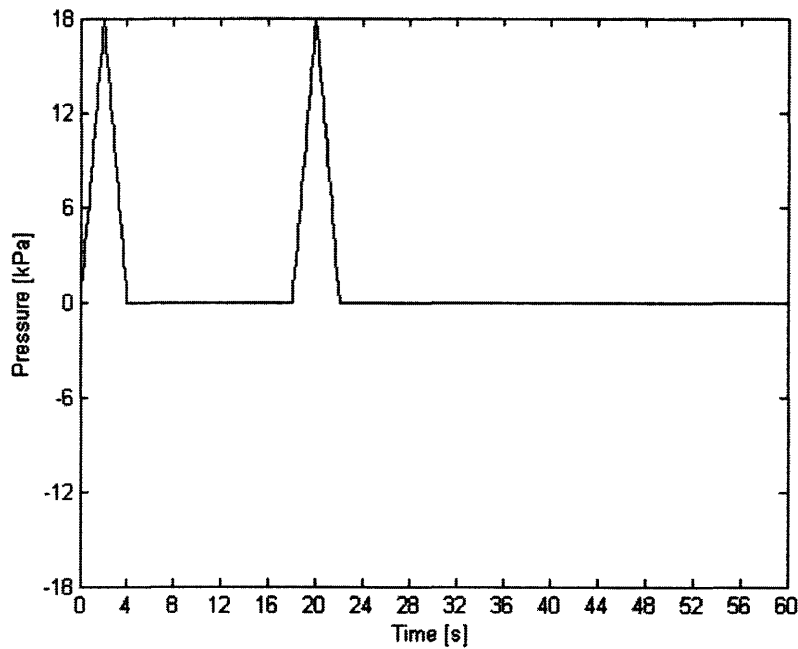


**Figure 16: Load Function 2:** This figure shows the second load function  $p$  applied to the cantilever beam.

The acceleration solutions for each scheme using a time step of 0.11 seconds and 0.22 seconds can be seen in Figures 17 and 20 respectively. The behavior of each scheme using load function 2 is consistent with their behavior using load function 1. The trapezoidal rule fails using each time step. It fails sooner using a time step of 0.22 seconds than with a time step of 0.11 seconds similar to what was seen using a single pulse load function. In addition, the percentage total error for the composite method steadily increases by small amounts, while the percentage total error quickly increases for the trapezoidal rule to magnitudes greater than 12,000% and 16,000% for a time step of 0.11 seconds and a time step 0.22 seconds respectively. The percentage total error for the composite method and the trapezoidal rule using a time step of 0.11 seconds can be seen in Figures 18 and 19 respectively. The percentage total error for the composite method and the trapezoidal rule using a time step of 0.22 seconds can be seen in Figures 21 and 22 respectively.

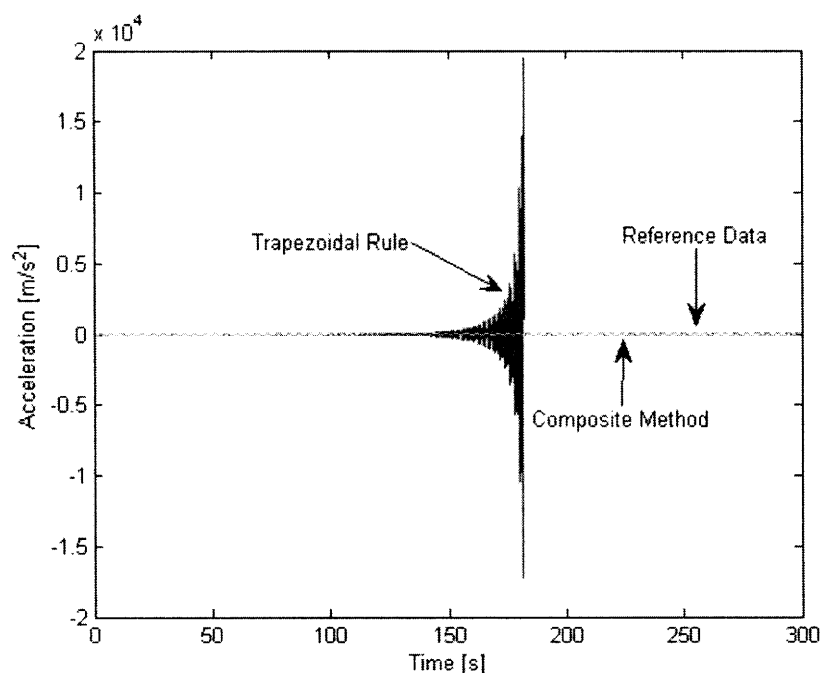


**Figure 17: Load Function 2-Time Step 0.11s-Acceleration vs Time Plot:** This figure shows that for a time step equal to 0.11s, the trapezoidal rule fails; whereas the composite method remains stable.

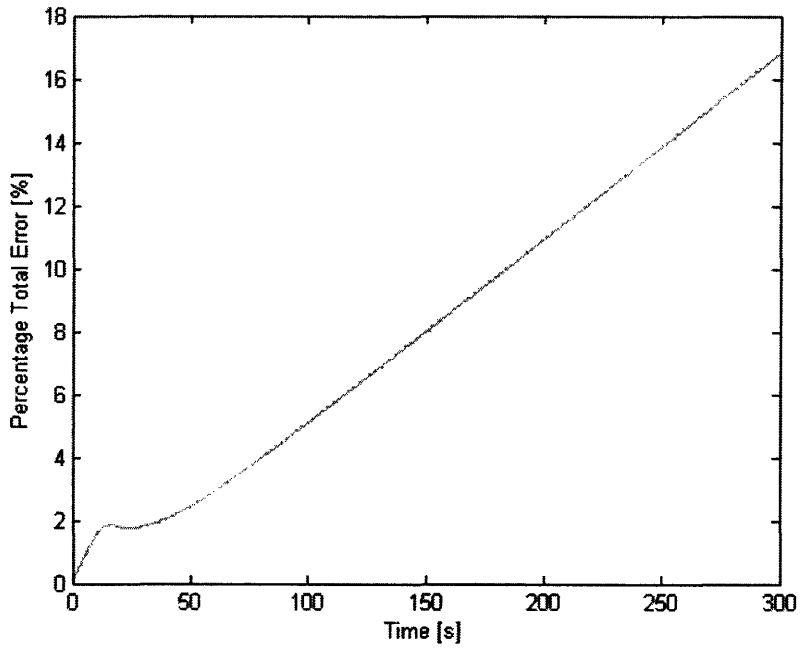


**Figure 18: Load Function 2-Time Step 0.11s-Composite Method Percentage Total Error:** This figure shows the percentage total error of the composite method as a function of time for a time step equal to 0.11s.

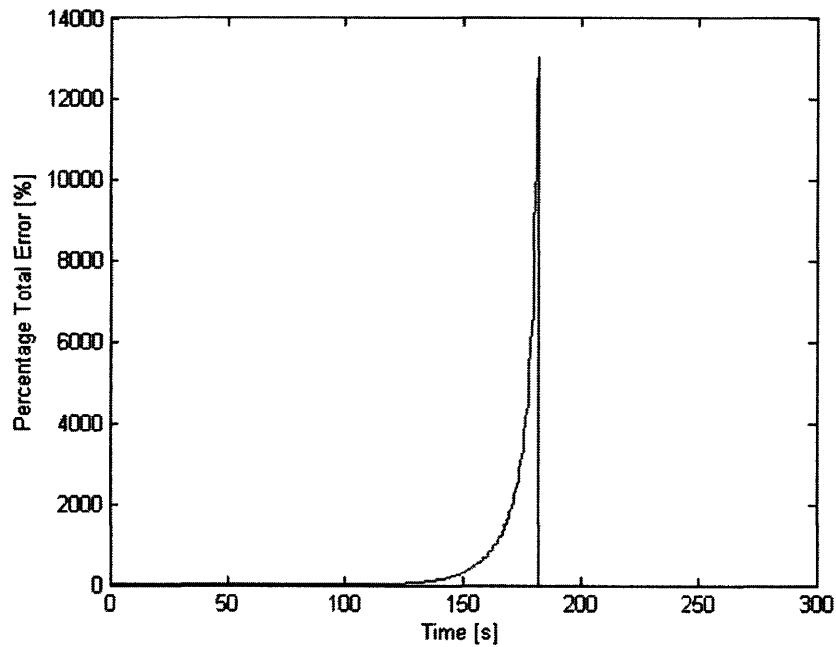


**Figure 19: Load Function 2-Time Step 0.11s-Trapezoidal Rule Percentage Total Error:** This figure shows the percentage total error of the trapezoidal rule as a function of time for a time step equal to 0.11s. The trapezoidal rule fails at time equal to 181.8s.

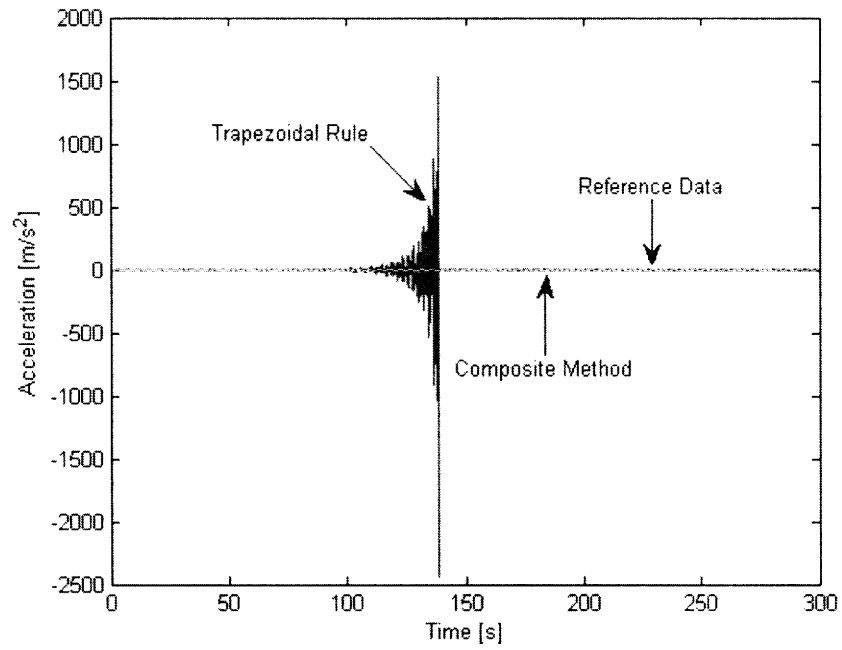


**Figure 20: Load Function 2-Time Step 0.22s-Acceleration vs Time Plot:** This figure shows that for a time step equal to 0.22s, the trapezoidal rule fails; whereas the composite method remains stable.

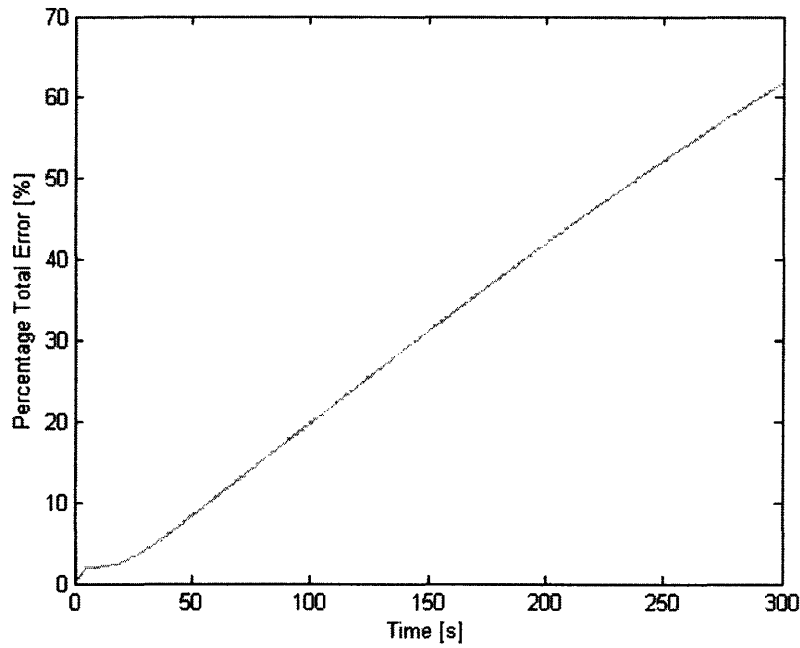


**Figure 21: Load Function 2-Time Step 0.22s-Composite Method Percentage Total Error:** This figure shows the percentage total error of the composite method as a function of time for a time step equal to 0.22s.

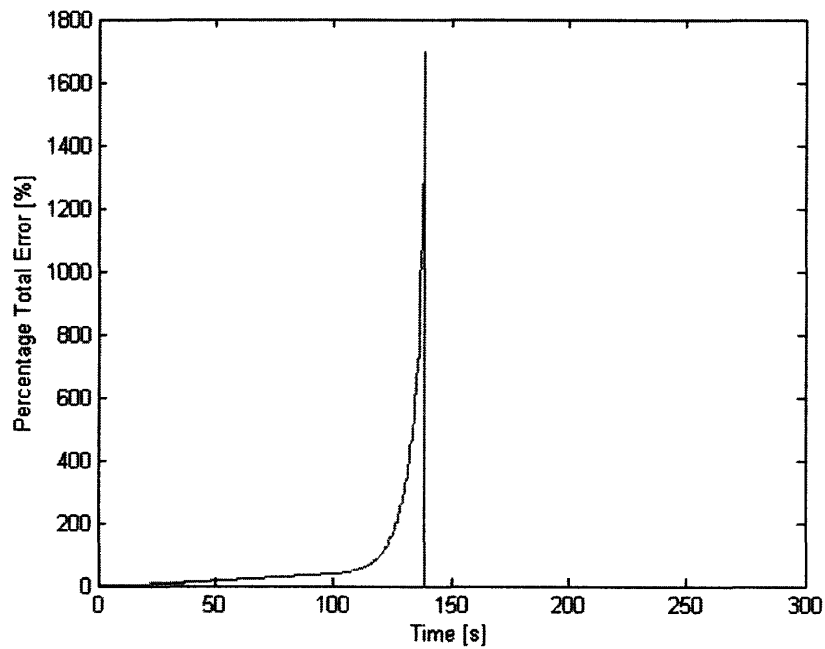


**Figure 22: Load Function 2-Time Step 0.22s-Trapezoidal Rule Percentage Total Error:** This figure shows the percentage total error of the trapezoidal rule as a function of time for a time step equal to 0.22s. The trapezoidal rule fails at time equal to 138.6s.

### 4.1.3 Triple pulse load function

The third load function (load function 3) used in this study was a triple pressure pulse whose first and second peaks were separated by 18 seconds and whose second and third peaks were separated by 20 seconds. The first and second pressure pulses were identical to the ones seen in load function 2 except that the second pressure pulse acts in the opposite direction. The third pressure pulse started at  $t = 38$  seconds, peaked at  $t = 40$  seconds, and ended at  $t = 42$  seconds. This third pressure pulse acted in the same direction as the first pressure pulse. Load function 3 can be seen in Figure 23. The magnitude of the peak pressure in each pulse was 18kPa. The pressure applied to the beam at any time  $t > 42$  seconds was zero.

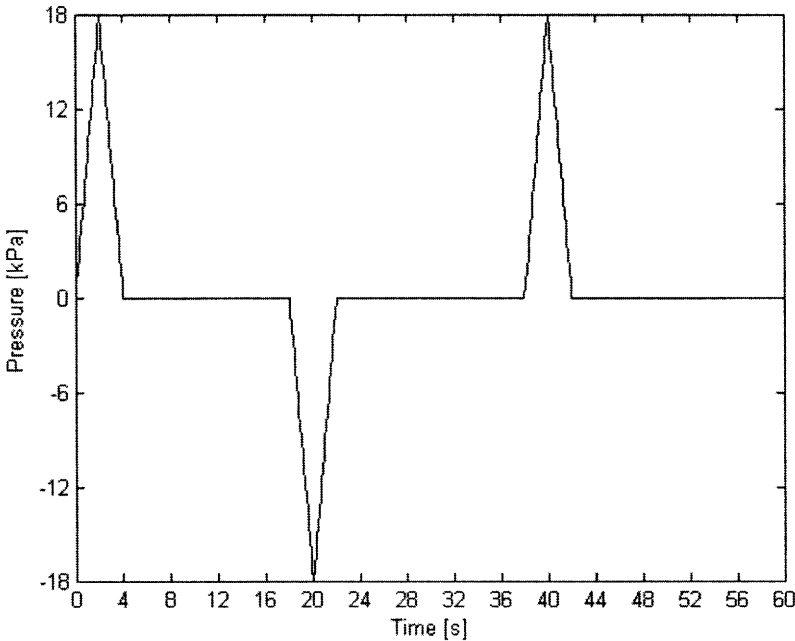


**Figure 23: Load Function 3:** This figure shows the third load function  $p$  applied to the cantilever beam.

The analysis shows that the acceleration solutions calculated from each scheme using load function 3 are consistent with the behavior seen using load function 1 and load function 2. The trapezoidal rule fails while the composite method remains stable, and the percentage total error for the composite method increases steadily by small amounts while the percentage total error for the trapezoidal rule increases rapidly to magnitudes

greater than 12,000% and 750% of the maximum magnitudes of acceleration found in the reference data for time steps of 0.11 seconds and 0.22 seconds respectively.

The acceleration solutions for the trapezoidal rule and the composite method for a time step of 0.11 seconds can be seen in Figure 24. The reference data cannot be seen due to the scale of the trapezoidal rule's failure. The composite method's data line covers it up since they are of the same magnitude. The acceleration solutions for a time step of 0.22 seconds can be seen in Figure 27. The percentage total error for the composite method and the trapezoidal rule using a time step of 0.11 seconds can be seen in Figures 25 and 26 respectively. The percentage total error for the composite method and the trapezoidal rule using a time step of 0.22 seconds can be seen in Figures 28 and 29 respectively.

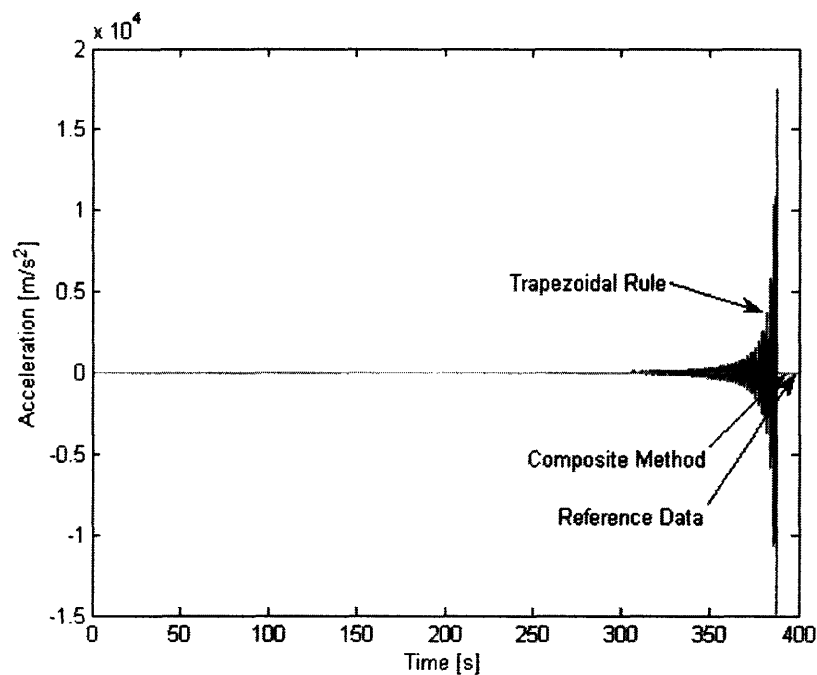


**Figure 24: Load Function 3-Time Step 0.11s-Acceleration vs Time Plot:** This figure shows that for a time step equal to 0.11s, the trapezoidal rule fails; whereas the composite method remains stable.

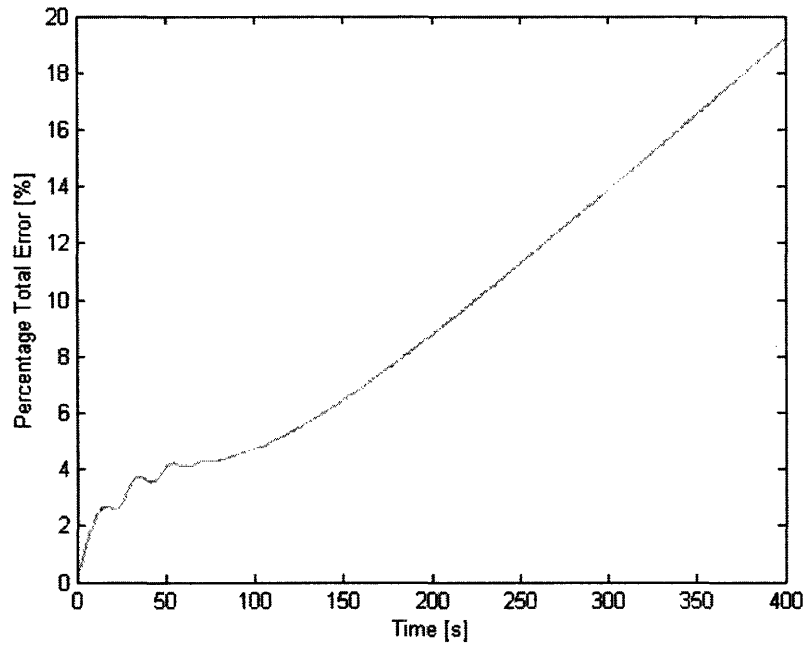


**Figure 25: Load Function 3-Time Step 0.11s-Composite Method Percentage Total Error:** This figure shows the percentage total error of the composite method as a function of time for a time step equal to 0.11s.

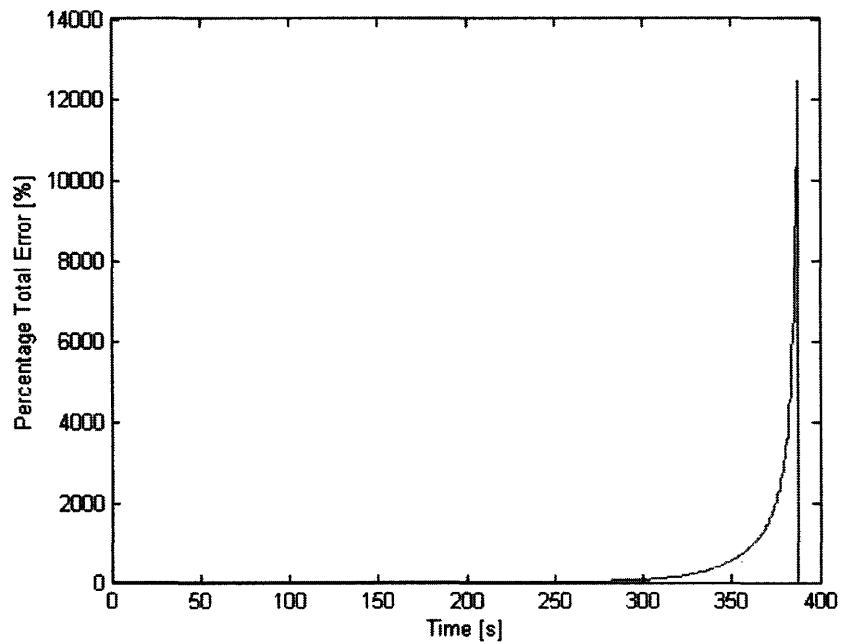


**Figure 26: Load Function 3-Time Step 0.11s-Trapezoidal Rule Percentage Total Error:** This figure shows the percentage total error of the trapezoidal rule as a function of time for a time step equal to 0.11s. The trapezoidal rule fails at time equal to 387.6s.



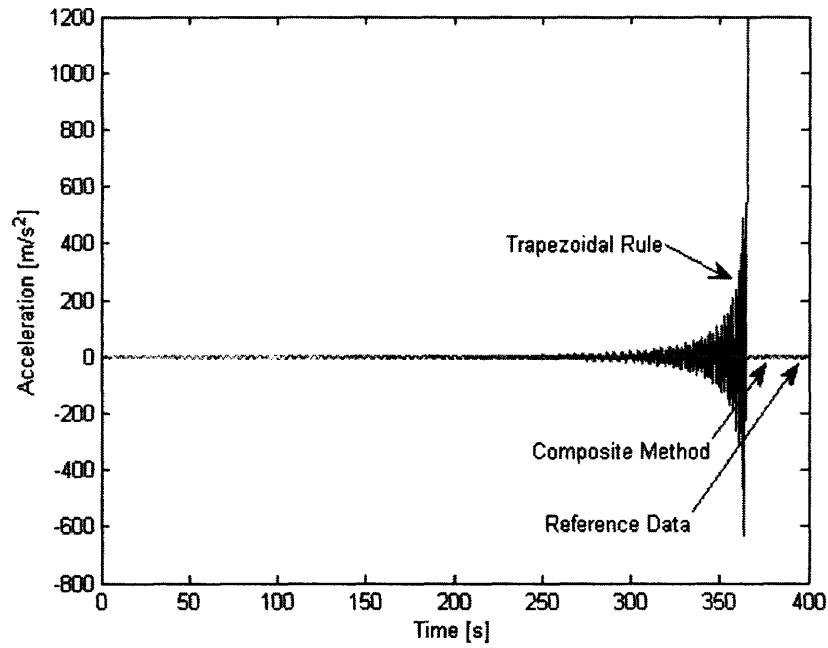


**Figure 27: Load Function 3-Time Step 0.22s-Acceleration vs Time Plot:** This figure shows that for a time step equal to 0.22s, the trapezoidal rule fails; whereas the composite method remains stable.

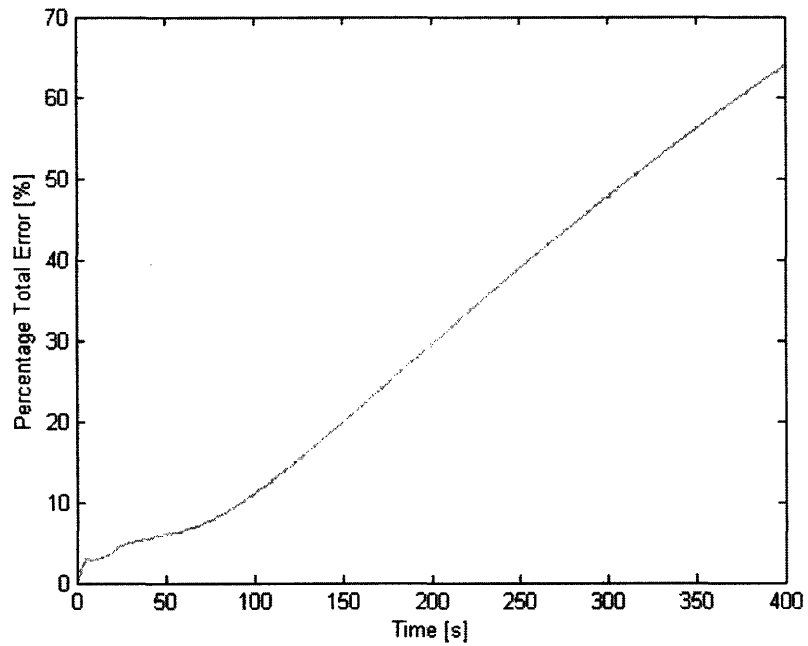


**Figure 28: Load Function 3-Time Step 0.22s-Composite Method Percentage Total Error:** This figure shows the percentage total error of the composite method as a function of time for a time step equal to 0.22s.

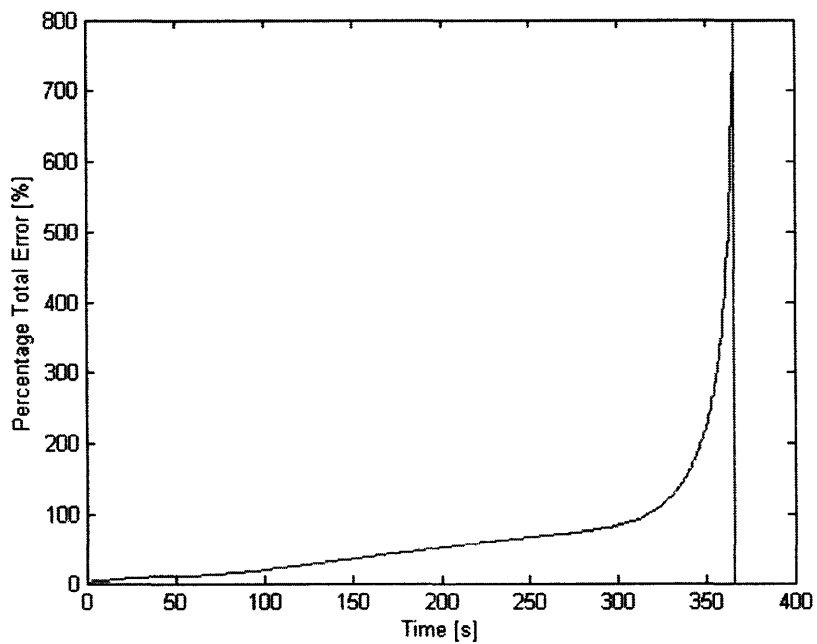


**Figure 29: Load Function 3-Time Step 0.22s-Trapezoidal Rule Percentage Total Error:** This figure shows the percentage total error of the trapezoidal rule as a function of time for a time step equal to 0.22s. The trapezoidal rule fails at time equal to 365s.

## 4.2 Beam whip analysis

The second problem evaluated in this study was an expansion of the first problem. It contains the same cantilevered beam, but it interacts with a physical obstruction 0.5m away from its tip as seen in Figure 30. The beam was divided into the same sixty nine-node plane stress elements as in problem 1 and the obstruction was modeled as a truss. In addition, the material properties of the beam remain consistent with problem 1. The Young's Modulus  $E = 2 \times 10^{11}$  Pa and Poisson's ratio  $\nu = 0.3$ . The truss is modeled as a nonlinear elastic material whose Young's Modulus  $E = 2.5 \times 10^{11}$  Pa. Additionally, the convergence tolerance criterion set in this analysis required that the energy for each iteration must have converged to within  $10^{-8}$  J of the original energy increment and the force for each iteration must have converged to within  $10^{-6}$  N of the original force increment.

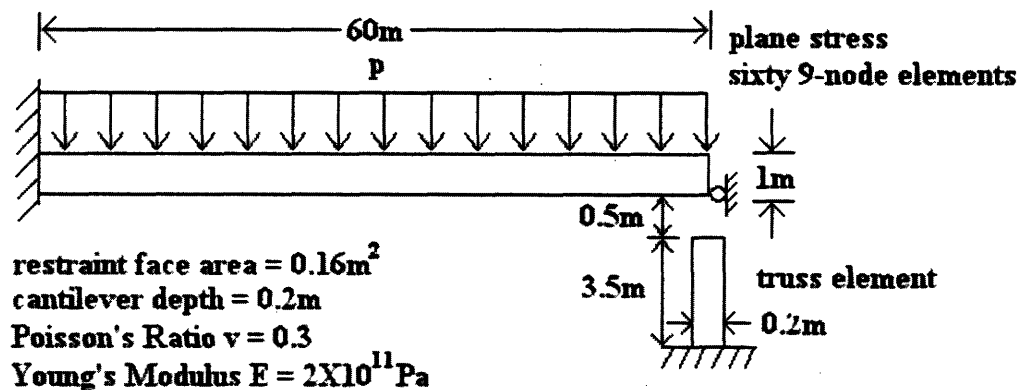


**Figure 30: Problem 2-Cantilevered Pipe Whip:** This figure shows the geometrical set up of the second problem. The Young's Modulus  $E$ , Poisson's ratio  $\nu$ , and thickness of the cantilever remain the same as in the first problem. In this problem, the cantilever contacts a restraint that is 0.5m from it. The restraint is modeled as a truss whose Young's Modulus  $E = 2.5 \times 10^{11}$  Pa and face area equals  $0.16\text{m}^2$ . The single pressure pulse  $p$  as used in this problem. It can be seen in Figure 2.

#### 4.2.1 Obtaining an “exact” reference solution

The original intent of this study was to subject the beam in problem 2 to all three of the same pressure loads  $\mathbf{p}$  seen in the first problem. This changed, however, after reviewing the solutions to this problem using the single pressure pulse  $\mathbf{p}$  used in problem 1. Figures 31, 32, and 33 show the “reference” solutions obtained for the displacement, velocity, and acceleration of this problem using a time step of 0.0044 seconds and a time step of 0.0022 seconds. These time steps correspond to 1/1000 and 1/2000 of the smallest mode period of the beam respectively. At such fine time steps, the calculated results should have reached an “exact” solution for the problem. However, this is not the case. Although the difference in the solutions for displacement is minimal, the difference in solutions for velocity increases, and the difference in solutions for acceleration are even greater. It is clear that an “exact” reference is difficult to obtain in this problem.

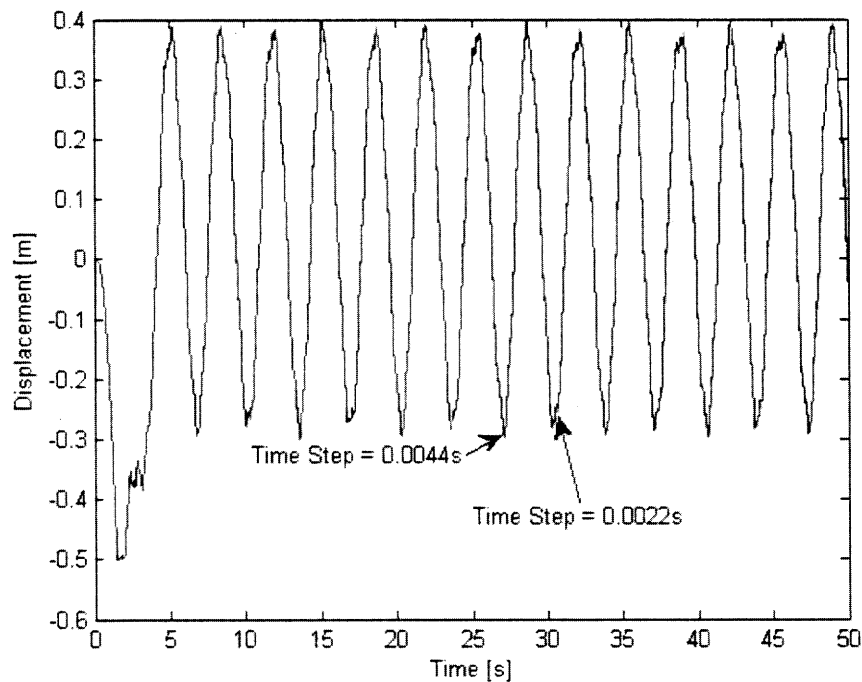


**Figure 31: Beam Whip “Reference” Displacement:** This figure shows the “reference” solutions calculated using different time steps for the displacement of the tip of the beam in problem 2.

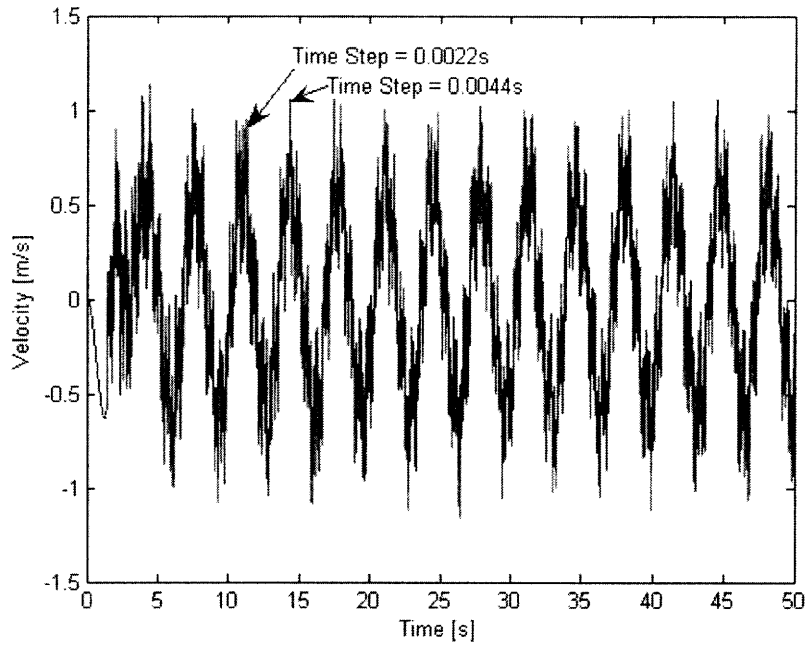


**Figure 32: Beam Whip “Reference” Velocity:** This figure shows the “reference” solutions calculated using different time steps for the velocity of the tip of the beam in problem 2.

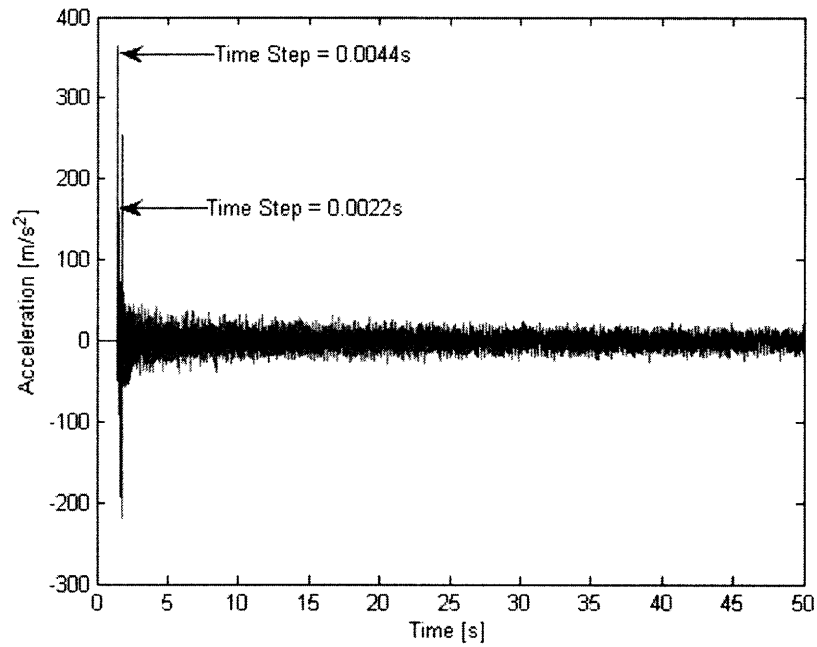


**Figure 33: Beam Whip “Reference” Acceleration:** This figure shows the “reference” solutions calculated using different time steps for the acceleration of the tip of the beam in problem 2.

#### 4.2.2 Single pulse load function

The behavior of the trapezoidal rule and the composite method can be observed by obtaining the solutions for displacement, velocity, and acceleration of the tip of the beam for each scheme. Although a true “exact” reference solution cannot be calculated, a “reference” solution was obtained by evaluating the problem with a time step of 0.0044s. This “reference” solution was used for visual comparison only. The solutions for the trapezoidal rule and the composite method were calculated using a time step of 0.11s.

The solution of displacements for the tip of the beam can be seen in Figure 34. The trapezoidal rule and the composite method correspond well with the “reference” solution. All three solutions seem to match almost perfectly until contact is made with the restraint.

The solution of velocities for the tip of the beam can be seen in Figure 35. The trapezoidal rule and the composite method correspond well with the “reference” solution until contact is made with the restraint. After this contact, the smooth line that was present before is now a line that jumps around frequently. The solutions do not match very well anymore.

The solution of accelerations for the tip of the beam can be seen in Figure 36. As seen in the solution of velocities and accelerations, the trapezoidal rule and the composite method correspond well with the “reference” solution until contact is made with the restraint. After this contact, the “reference” data shows a spike in the acceleration that the trapezoidal rule and the composite method do not see. The trapezoidal rule and the composite method do not oscillate at the same level of magnitude as the “reference” data. After contact with the restraint, the “reference” data shows large oscillations that settle to smaller oscillations about equilibrium. The trapezoidal rule and the composite method never show large oscillations. However, the oscillations that the trapezoidal rule experiences are of the same magnitude as the oscillations that the “reference” data settles to; while the oscillations that the composite method predicts are much smaller.

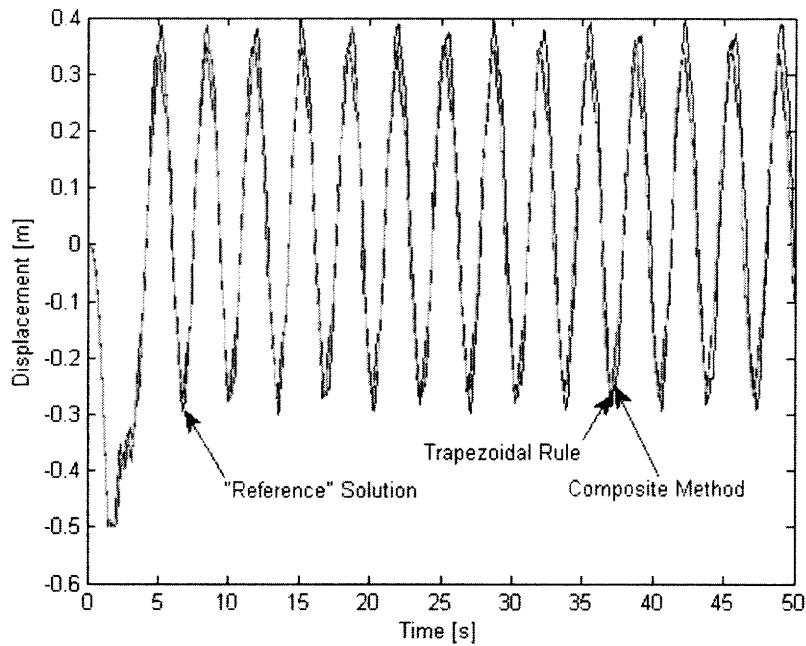


**Figure 34: Beam Whip-Time Step 0.11s-Displacement vs Time Plot:** This figure shows the displacement solutions obtained for the tip of the beam by using a time step of 0.0044s for the “Reference” solution and 0.11s for the other schemes.

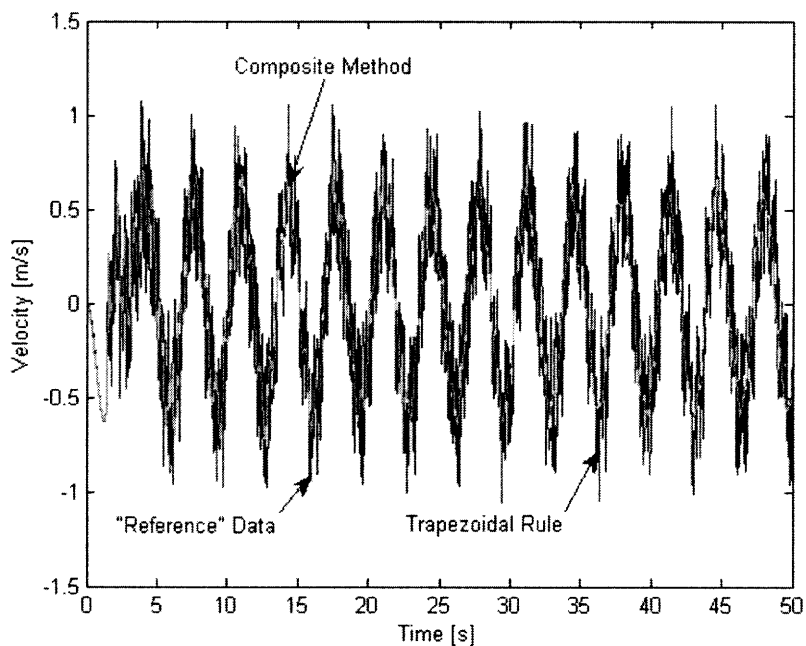


**Figure 35: Beam Whip-Time Step 0.11s-Velocity vs Time Plot:** This figure shows the velocity solutions obtained for the tip of the beam by using a time step of 0.0044s for the “Reference” solution and 0.11s for the other schemes.

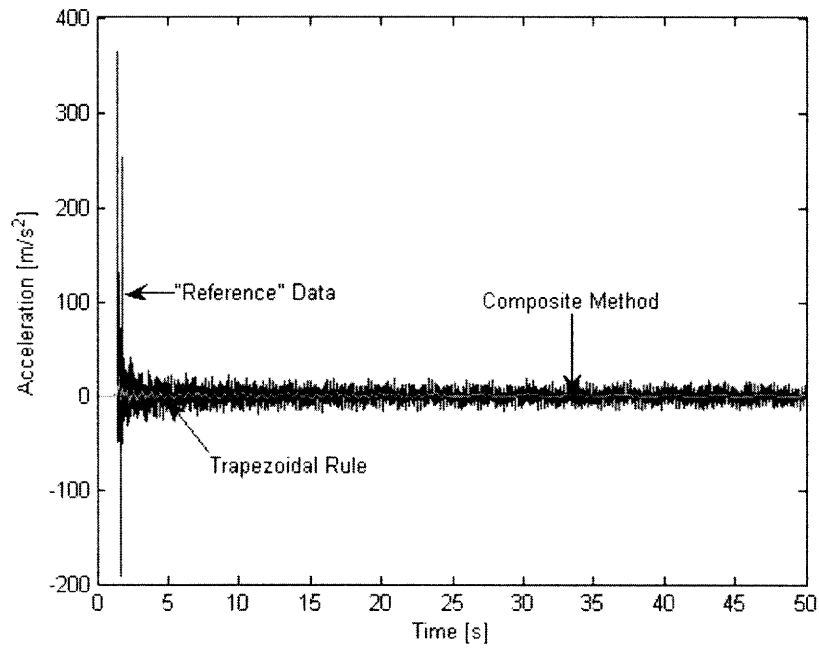


**Figure 36: Beam Whip-Time Step 0.11s-Acceleration vs Time Plot:** This figure shows the acceleration solutions obtained for the tip of the beam by using a time step of 0.0044s for the “Reference” solution and 0.11s for the other schemes.



## Chapter Five: Conclusions

The purpose of this study was to compare the trapezoidal rule and the new composite method in order to determine which scheme produced more accurate results. The integration schemes were compared by solving for the accelerations of a large displacement nonlinear problem, and by solving for the displacement, velocity, and acceleration profiles of a contact nonlinear problem. Different time steps and loading functions were applied in order to obtain a better understanding of how each scheme responds under different situations.

In all cases of the large displacement problem (problem 1), the composite method remained stable whereas the trapezoidal rule experienced a complete failure. This complete failure consisted of the percentage total error in the acceleration solution increasing rapidly to errors as great as 16,330% of the maximum actual acceleration before completely failing. The composite method, on the other hand, showed no signs of beginning to fail and produced fairly accurate results. The greatest error to occur for the composite method over a time range of 300 seconds was 62% of the maximum actual acceleration using a time step of 0.22 seconds (time step 2). The greatest composite method error that occurred using a time step of 0.11 seconds (time step 1) was only 17% of the maximum actual acceleration.

The main conclusion that can be drawn from the study of the contact nonlinear problem (problem 2) is that further study must be done in order to fully understand the problem. The composite method was the direct time integration scheme used in this study to find the reference data in all cases of each problem. However, the composite method failed to converge to an “exact” solution when taking a time step equal to 1/1000 of the smallest mode period for the second problem. In addition, both the composite method and the trapezoidal rule failed to detect the large increase in acceleration seen by the beam tip after contact with the restraint material was made. Also, the magnitude of the composite method acceleration solution appeared noticeably smaller than the “reference” magnitude

of acceleration. The magnitude of the trapezoidal rule acceleration solution was similar to the “reference” magnitude after it had settled about equilibrium.

Another aspect to consider in this study is the computational effort required to use each integration scheme. Since the composite method is a two step scheme and the trapezoidal rule is a single step scheme, the composite method takes twice as long as the trapezoidal rule to calculate a solution. In order for the composite method to be considered better than the trapezoidal rule, this extra time cost should be justified by the results in the solutions obtained. The results from the large displacement problem (problem 1) would indicate that the composite method remains stable while the trapezoidal rule fails completely. So any solutions obtained from the trapezoidal rule would be of no value. Therefore, in cases where accurate results are needed, it is justified to use the more time consuming composite method. However, results from the contact problem (problem 2) show that further study is needed of the composite method when used in contact problems.

## References

- [1] Bathe KJ. Finite Element Procedures. New York: Prentice Hall; 1996.
- [2] Collatz L. The Numerical Treatment of Differential Equations. Third ed. New York: Springer-Verlag; 1966.
- [3] Bathe KJ, Baig MMI. On a Composite Implicit Time Integration Procedure for Nonlinear Dynamics. *Computers & Structures* 2005; 83:2513-2524.
- [4] Bathe KJ. Conserving Energy and Momentum in Nonlinear Dynamics: A Simple Implicit Time Integration Scheme. *Computers & Structures* 2007; 85:437-445.
- [5] Chung J, Hulbert GM. A Time Integration Algorithm for Structural Dynamics with Improved Numerical Dissipation: The Generalized Alpha method. *J Appl Mech, Trans ASME* 1993; 60:371-5.
- [6] Wilson EL, Farhoomand I, Bathe KJ. Nonlinear Dynamic Analysis of Complex Structures. *Int J Earthquake Eng Struct Dyn* 1973; 1:241-52.
- [7] Bathe KJ. On Reliable Finite Element Methods for Extreme Loading Conditions. In: Ibrahimbegovic A, Kozar I, editors. *Extreme Manmade and Natural Hazards in Dynamics of Structures*. Springer Verlag; in press.
- [8] Kojic M, Bathe KJ. *Inelastic Analysis of Solids and Structures*. Springer; 2005.
- [9] Bathe KJ, Cimento AP. Some Practical Procedures for the Solution of Nonlinear Finite Element Equations. *J Comput Meth Appl Mech Eng* 1980; 22:59-85.
- [10] Grätsch T, Bathe KJ. A Posteriori Error Estimation Techniques in Practical Finite Element Analysis. *Comput Struct* 2005; 83:235-65.